1975

An improved model of emulsion polymerization

Robert William Thompson
Iowa State University

An improved model of emulsion polymerization

by

Robert William Thompson

A Dissertation Submitted to the
Graduate Faculty in Partial Fulfillment of
The Requirements for the Degree of
DOCTOR OF PHILOSOPHY

Department: Chemical Engineering and Nuclear Engineering
Major: Chemical Engineering

Approved:

Signature was redacted for privacy.

In Charge of Major Work

Signature was redacted for privacy.

For the Major Department

Signature was redacted for privacy.

For the Graduate College

Iowa State University
Ames, Iowa

1975

TABLE OF CONTENTS

NOMENCLATURE

A_T	total polymer surface area, cm^2/cm^3
$A_1, A_2, \ldots, A_7$	constants in population balance model, dimensionless
a	surface area of a polymer particle, cm^2
C	constant of integration, dimensionless
d	particle diameter, cm
d_0	diameter of a micelle, cm
F	initiator efficiency, dimensionless
f	generating function defined by Equation 2, $\#/v^2$
g	function describing particle size data defined by Equation 57, dimensionless
$I_{0,1}$	feed, effluent concentration of initiator, gm mole/liter
K	particle growth rate constant, cm^3/hr
K_j	corresponding rate constant multiplied by residence time in the reactor
k_d	initiator decomposition rate constant, 1/hr
k_i	initiation rate constant, cm^3/gm mole hr
k_p	polymerization rate constant, cm^3/gm mole hr
k_t	termination rate constant, cm^3/gm mole hr
k_v	rate constant describing loss of micelles to polymer particle surfaces, cm^3/gm mole hr

k_o	desorption rate constant, dimensions depend on model: Sato-Taniyama model, 1/hr; population balance model, cm/hr
M_m	monomer concentration in the polymer particles, gm mole/cm^3
M_w	molecular weight of monomer, gm/gm mole
$M_{0,1}$	feed, effluent concentration of monomer, gm mole/cm^3
$m_{0,1}$	feed, effluent concentration of micelles, gm mole/cm^3
N	total concentration of polymer particles, gm mole/cm^3
N_A	Avogadro's number, molecules/gm mole
N_n	number density of polymer particles having n radicals, $\#/v^2$ ($N_n dv$ is the concentration of particles having n radicals between sizes v and v+dv)
$N_T = \sum_{n=0}^{\infty} N_n$	overall number density of polymer particles, $\#/v^2$
N_{T_0}	number density of polymer particles at "zero size," $\#/v^2$
N_1	effluent concentration of dead particles, gm mole/cm^3
N_1^*	effluent concentration of live particles, gm mole/cm^3
n	number of free radicals present in a polymer particle, dimensionless
$\bar{n}$	average number of radicals per particle, dimensionless
$\bar{n}_s$	overall system average number of radicals per particle, dimensionless

n_T	total number of active free radicals in the polymer particles, dimensionless
$P = \int_1^\infty X_T d\zeta$	dimensionless total concentration of particles leaving the reactor
$P' = \int_1^\zeta X_T d\zeta$	dimensionless cumulative concentration of polymer particles leaving the reactor
p, r	parameters in Stockmayer's solution, dimensionless
q	volumetric flow rate through the system, cm^3/hr
$R = \int_1^\infty n_T d\zeta$	dimensionless total number of growing polymer chains leaving the reactor
$R' = \int_1^\zeta n_T d\zeta$	dimensionless cumulative number of growing polymer chains leaving the reactor
R_p	rate of polymerization, gm mole/cm^3hr
R_{v_n}	growth rate for the N_n-type particle, cm^3/hr
R*	effluent concentration of free radicals, gm mole/cm^3
r_{N_n}	rate of formation of the N_n-type particle, $\#/v^2hr$
S	total surface area of particles and micelles, cm^2/cm^3
S_c	amount of soap covering polymer particles, gm mole/cm^3
$S_{0,1}$	feed, effluent concentration of soap, gm mole/cm^3
S_9	number of soap molecules per micelle, dimensionless
s	space time for plug flow reactor, hr
t	time, hr
V	system volume, cm^3

v	particle volume, cm^3
v_0	micelle volume, cm^3
X_n	dimensionless number density for the N_n-type particle
X_T	dimensionless overall number density for polymer product
x	dummy variable in Equation 9, dimensionless
x_1, x_2, x_3	system coordinates, length

Greek symbols:

α, β, γ	constants defined by Equation 28
ϵ	parameter defined in Table 5, dimensionless
ζ	dimensionless particle volume coordinate
ρ_A	rate of radical production, $\#/cm^3 hr$
ρ_m, ρ_p	monomer, polymer densities, respectively, gm/cm^3
σ, σ'	dimensionless constants in Equations 5 and 8, respectively
η	dummy variable introduced in Equation 2, dimensionless
τ	average residence time, hr
ϕ_M	volume fraction of monomer in polymer particles, dimensionless
Ψ	conversion of monomer, dimensionless

INTRODUCTION

The production of polymers now represents a sizeable fraction of American industry. New applications for polymeric materials are continually being found. The interest in polymers arises largely because of their unique physical properties which are a result of their high molecular weights. These molecular weights are a consequence of the manner in which polymers are made. It is indirectly these characteristic properties and their prediction that will be of concern here.

Historical Perspective

A brief look at the history of polymers and polymer chemistry is a most fascinating one. As common as polymers are today, and as vital as natural polymers are to our existence, the concept of a macromolecule was not accepted among the "learned" until the 1920's. The macromolecular concept was set forth chiefly by Hermann Staudinger during this period, but he received violent resistance to the idea (Billmeyer (3)):

> "Dear Colleague, Leave the concept of large molecules well alone...there can be no such thing as a macromolecule."

In the 50 years since that period we have come to accept, and understand somewhat, the notion of a polymer. The concept of monomer units, i.e. molecular building blocks, reacting in such a way as to yield relatively large chemical structures explains many of the strange phenomena reported by chemists and physicists over a century ago. There were reported to be certain colloidal substances which had negligible diffusion rates in solution, would not pass through semipermeable

membranes, and had extremely large molecular weights. Some of these materials had extraordinary strength and exhibited strange rheological properties (6).

The earliest research done in the field of polymer chemistry was the study of naturally occurring polymers, rubber and starch being the prime targets of investigation. By the mid-1800's hard rubber was sold commercially in this country. Cellulose nitrate was made available by 1870, and by 1907 purely synthetic phenolic resins (phenol-formaldehyde copolymers) and varnishes were marketed. This was the birth of the synthetic plastics industry. Poly(vinyl chloride-acetate) production started in the 1920's. Polystyrene was produced commercially in the United States in the late 1930's (3).

There exist four basic techniques for polymer production: bulk, solution, suspension, and emulsion. These processes differ in the chemical recipe used and the location of the reactions in the polymer system. Each method has inherent advantages and disadvantages (3), and in addition, polymers made by different techniques may have widely different characteristics. Of concern here is the process of emulsion polymerization.

The importance of emulsion polymerization was realized during World War II, when the production of rubber became very crucial. Since then, emulsion polymerization has become a major industrial process for the manufacture of such products as: paint latex, textiles, adhesives, coatings, floor polishes and finishes, synthetic rubber, and countless other items.

Several distinct phases are present during the emulsion polymerization process. Water is frequently used as a carrying medium and a solvent for the inorganic initiator of free radicals. The water forms the "outer phase" of the emulsion. The monomer to be polymerized is stabilized by emulsifier molecules, which contain both hydrophobic and hydrophilic end groups. The emulsified monomer forms the "inner phase" of the emulsion. The excess emulsifier molecules (soap molecules) form clusters of molecules called micelles. Micelles vary in shape and size depending on the soap used, but in general consist of 50-100 soap molecules in a cluster which might be 50-100 Å in diameter (6). The monomer, being slightly soluble in water, will release molecules from the droplets to the outer phase. These molecules eventually find their way into the micelles, where the bulk of the polymerization will occur after a micelle has been stung by a radical from the outer phase. Polymerization initiated in the micelles then generates discrete particles containing monomer and polymer surrounded by the soap molecules which were once micelles. New particles may be formed as long as micelles exist. As polymerization proceeds, monomer continues to diffuse from the droplets through the outer phase to the growing polymer particles. Polymerization will occur until there are no free radicals remaining, or until the monomer is consumed.

The fact that polymerization begins in the micelles sets emulsion polymerization apart from the other polymerization techniques. This process has the advantages of high polymerization rates, high molecular weight products, easy heat removal and control, and easily handled products. The latex product is sometimes marketed without further processing.

These broad concepts of emulsion polymerization were first proposed by Harkins (16) in 1947. His conceptual picture has remained essentially unchanged to the present day, although there has been some evidence presented to support the theory that particle nucleation occurs in the water phase while polymer particles are merely stabilized by soap molecules (28). Flory (6) presents an excellent discussion of emulsion polymerization in his book.

Batch Reactor Analysis

Chemists, being more inclined to use batch reactors to study reaction mechanisms, began the investigation of polymer chemistry in batch systems. The batch reactor is somewhat easier to operate than a continuous reactor, and the quantity of chemicals required is much less for a batch than for a continuous system. Much has been learned from these studies which must be reviewed before proceeding to continuous reactors, especially because some of the results from the batch studies will be used in proceeding with the investigation of continuous emulsion polymerization.

The conceptual picture presented by Harkins (16) was first treated mathematically by Smith and Ewart (33) in 1948. They developed a "steady state" recursion relation for the transfer of free radicals between the outer phase and the polymer particles. This recursion relation was nothing more than a steady state material balance for a particular type of polymer particle, characterized by the number of free radicals present in the particle. Because the Smith-Ewart work is so often cited and used in analysis, it is necessary to fully understand it.

Smith and Ewart suggested (after Harkins) that free radicals from the water phase may enter a polymer particle which had no radicals present and initiate polymerization of the monomer contained therein. Upon the arrival of a second radical, a second chain could be initiated, or mutual termination of the two radicals could occur. A free radical has the option of desorbing from the particle and reentering the water phase. In principle, a polymer particle may house any number of free radicals, depending on the size of the particle and the magnitudes of the competing mechanisms.

The steady state Smith-Ewart recursion relation is written as follows:

$$\frac{k_t}{N_A v}\left\{(n+2)(n+1)N_{n+2} - n(n-1)N_n\right\} + \frac{\rho_A}{N}\left\{N_{n-1} - N_n\right\} + \frac{k_o a}{v}\left\{(n+1)N_{n+1} - nN_n\right\} = 0, \tag{1}$$

where:

a = surface area of a particle

k_t = termination rate constant

k_o = desorption rate constant

N_n = concentration of particles having n radicals

N = total concentration of particles

n = number of free radicals in a particle

v = particle volume

ρ_A = rate of generation of free radicals

Values of n are the set of non-negative integers. It is understood that negative subscripted variables are non-existent and their values set equal

to zero. The three bracketed terms represent the mechanistic steps of termination, absorption, and desorption of free radicals, respectively. As seen here, the termination mechanism is inversely proportional to particle volume, absorption is independent of volume, and desorption of free radicals is proportional to surface area and inversely proportional to particle volume. These relationships will be refined later. (Note that because previous workers considered no particle size distributions in their batch systems, the N_n functions in Equation 1 represent particle concentrations. These functions may equally well represent number densities of polymer particles when the particle size variation is considered. No significant ambiguities are introduced in this context.)

The batch emulsion polymerization process is usually divided into three time periods (8). During the first period the micelles are being depleted with the formation of polymer particles. This induction period is usually small compared to the whole batch process. Once micelles no longer exist the total number of particles remains constant as polymerization proceeds. This phase is the second time period. The disappearance of the monomer droplets marks the beginning of the third time period. Polymerization during this period consumes the residual monomer in the system and, as a result, proceeds at an ever decreasing rate. The Smith-Ewart recursion relation describes free radical transfer during the second time period, when the number of particles is fixed and emulsified droplets of monomer exist in the system.

Once having derived the recursion relation, Smith and Ewart solved it for three limiting cases. Their case II kinetics are most frequently

cited, and occur when the desorption mechanism is inoperative. In addition, the polymer particles are allowed to house a maximum of one free radical, because it is assumed the arrival of a second radical causes immediate mutual termination of the two radicals, and consequently polymer growth stops. They showed that, on the average, half of the particles are void of radicals at any time, while the other half contain one growing chain in each particle. Free radicals enter active and inactive particles at the same rate, thus maintaining the average number of radicals per particle, $\bar{n}_s$, at a constant value of 0.5. Reference made to the "Smith-Ewart theory" usually implies their case II kinetics, wherein $\bar{n}_s = 0.5$.

Much progress has been made since the Smith-Ewart study. Stockmayer (36) employed a generating function and was able to solve the recursion relation exactly for any real positive values of the mechanistic parameters. His expression for $\bar{n}_s$ involved a ratio of modified Bessel functions. While Stockmayer's solution was correct when desorption of radicals was absent, he erred in his solution when the desorption mechanism was present (J. T. O'Toole, ARCO Chemical Company, Glendale, Pennsylvania, personal communication, 1973.).

O'Toole (22) emended Stockmayer's error and presented the correct solution for $\bar{n}_s$. The technique utilized by both Stockmayer and O'Toole was to introduce the generating function, f:

$$f(\eta) \equiv \sum_{n=0}^{\infty} N_n \eta^n \qquad (2)$$

where η was merely a dummy variable. Each term in Equation (1) is then proportional to the function f or its first or second derivative with

respect to the dummy variable, η. By making the proper substitutions, Stockmayer derived the following ordinary differential equation:

$$(1+\eta)f''(\eta) + pf'(\eta) - rf(\eta) = 0, \tag{3}$$

where:

$$p = \frac{k_0 a N_A}{k_t} \quad \text{and} \quad r = \frac{\rho_A N_A v}{N k_t},$$

and where the primes denote differentiation with respect to η. Because there were no appropriate boundary conditions for this differential equation, meaningful results were limited to the evaluation of the quantity $\bar{n}_s$:

$$\bar{n}_s = \frac{f'(\eta)_{/\eta=1}}{f(\eta)_{/\eta=1}}. \tag{4}$$

O'Toole correctly determined this quantity to be:

$$\bar{n}_s = \frac{\sigma}{4} \frac{I_p(\sigma)}{I_{p-1}(\sigma)}, \tag{5}$$

where: $\sigma^2 = 8r$,

and where the I's are the modified Bessel functions. O'Toole plotted results showing how $\bar{n}_s$ varied with p and σ. Inherent in these parameters is the variation of $\bar{n}_s$ with particle size (i.e. the particle volume). These results are <u>not</u> to be construed as yielding anything analogous to a particle size distribution, for the distribution of particle sizes was initially assumed to be a "spike," i.e. all particles were assumed to be uniform in size. What this model allows is that the whole collection of uniform sized particles grows uniformly with time in the batch reactor environment, even though this growth rate may not be predicted by this

theory.

Ugelstad et al. (39) set forth the proposition that free radical desorption and absorption are not independent processes if the desorbed radicals may be reabsorbed by polymer particles. These mechanisms are independent only if a desorbed free radical becomes inactive as a result of the desorption process. They allowed the absorption of free radicals to depend on radical desorption and provided a numerical solution to the same problem solved by Stockmayer and O'Toole.

Gardon has recently published an excellent review of the state of the art of emulsion polymerization (8-13). He included a review of the Smith-Ewart development, a summary of the data available in the literature, and some original work in the field. Of prime importance here is his article (10) in which he reexamined the Stockmayer solution for the case of no desorption. Gardon realized that the batch reactor is never at "steady state," even though the total number of particles may remain constant throughout the second and third time periods. Gardon retained the time derivative term associated with the process and obtained a numerical solution to the resulting problem. When he compared his numerical results to Stockmayer's (neglecting desorption) the deviation was curiously minimal. This observation may suggest that the time derivative term was of negligible importance in his calculations.

While many researchers have worked with the Smith-Ewart concept of emulsion polymerization, there have also been some different approaches to the problem. Sato and Taniyama (31) treated emulsion polymerization as if there were a bimolecular reaction occurring between polymer particles and

free radicals. They assumed that all polymer particles were the same size and that a particle could have either zero or one active radical. All active particles were assumed chemically identical; all inactive particles were assumed chemically identical. They allowed the possibility that active particles might capture free radicals from the outer phase at a different rate than the inactive particles, however, there is little evidence to warrant this generality. From their model resulted the first analysis and prediction of all active species in the polymerization system.

Katz, Shinnar, and Saidel (18) presented the results of a sophisticated mathematical model, which predicts molecular weights in a batch polymerizer. They treated the "steady state" case where the desorption mechanism was inoperative. After painstakingly rederiving the Smith-Ewart recursion relation and succumbing to Stockmayer's solution for $\bar{n}_s$, they were able to arrive at polymer size distributions in the particles, from which they calculated molecular weight distributions. Their mechanisms of radical capture, radical termination, and particle growth were all assumed independent of particle size, a rather primitive assumption on their parts. While their model was capable of predicting polymer sizes in a particle, they said virtually nothing about the particle size distribution in the batch system. Their model assumed a monodisperse latex. When they finally calculated results, they limited themselves to two extremes, the Smith-Ewart case II kinetics and bulk kinetics.

Two recent additions to the field were given by O'Toole (23) and Saidel and Katz (30). Both papers employed a stochastic approach to

analyze emulsion polymerization in a batch reactor. Both works neglected the desorption mechanism and both assumed that the polymer particles might contain zero or one free radical. (O'Toole's development permitted more than one radical to be present, but obtaining results for this case proved to be too formidable to warrant his further pursuit.) Saidel and Katz used moments of distributions to study the particle size variation in the polymer product.

Sundberg and Eliassen (37) used a population balance to predict both particle size and molecular weight distributions in a batch emulsion polymerizer. They ignored the mechanism of free radical desorption, and they allowed particles to house only one free radical at most. From their population balance they were able to predict particle size distributions, the conversion level of monomer, and the effluent micelle concentration. They did not evaluate their results with data, and the details of their work were excluded. No reference was made to other work done by the authors. Their model and results were largely unexplained.

Another school of thought is represented by Williams and his co-workers (41). All of the theories discussed thus far assume a uniformly mixed polymer particle (consisting of polymer and monomer), such that polymerization may take place anywhere inside the particle. Williams et al. proposed a core-shell morphology in which polymerization occurs on an outer shell of the particle, the inner core being essentially impermeable to the free radicals and the growing polymer chains. William's book (41) gives the reader an overview of this concept and provides more detailed references.

Continuous Stirred Tank Reactor Analysis

Oftentimes large scale productions of plastics will involve continuous operation, because of distinct inherent advantages of this process: product consistency, less manpower requirements, greater yields, etc. Any discussion leading to a new mathematical model would not be complete without a thorough review of the state of the art of continuous emulsion polymerization.

The first major contribution to the continuous emulsion polymerization literature was by Gershberg and Longfield (15). They applied Smith-Ewart case II kinetics to a continuous polymerizer. Their conclusions were consistent with the Smith-Ewart model, but the data they presented were not described well by their model. As their work was unpublished, the derivation was recapitulated by Gerrens and Kuchner (14).

Sato and Taniyama (32) applied the bimolecular reaction concept to continuous emulsion polymerization. This idea immediately followed from their earlier work (31). Their results were similar to those of Gershberg and Longfield, but more extensive. The results were consistent with the Smith-Ewart theory and exhibited some degree of flexibility in that the average number of radicals per particle, $\bar{n}_s$, need not be assigned the value of 0.5. These workers were the first ones to concern themselves with the effluent concentrations of the other components involved.

The principle behind the Sato-Taniyama model was extended by Nomura et al. (20). They were able to keep track of polymer chain length in addition to the free radical distribution. They presented some new results, but their model failed to describe the data accurately at low

residence times.

In the works on continuous emulsion polymerization discussed thus far, the desorption of free radicals and polymer particle size distribution have both been ignored. There have been investigations which attempted to include one or the other of these effects, but not both simultaneously.

Behnken et al. (1) described a technique for predicting size distributions in systems where particles were growing or shrinking. Funderburk (7) and Stevens and Funderburk (35) employed this population balance technique in an attempt to predict particle size distributions leaving a continuous emulsion polymerizer. Several growth rate models were tested; of particular interest was the Stockmayer model.

Funderburk's major contribution to the field of emulsion polymerization was to show how the population balance technique (frequently used in crystallization work (26, 27)) may be employed in analysis of particle sizes leaving a continuous stirred tank polymerizer. Describing the system on a particle volume basis, Funderburk arrived at:

$$\frac{\partial N_T}{\partial t} + \frac{\partial}{\partial v}(N_T R_{v_n}) + \frac{N_T}{\tau} = 0, \tag{6}$$

for the case of no particles in the feed stream. His N_T function was characterized as:

$$N_T = N_T(v,t,\bar{n}_s). \tag{7}$$

To describe N_T as a function of the variables involved was to describe the overall particle size distribution leaving the continuous reactor. Implicit in his N_T function was that N_T depended on the quantity $\bar{n}_s$ through the

growth rate function R_{v_n}. R_{v_n} for Funderburk was proportional to $\bar{n}_s$. Funderburk then proceeded to arrive at an expression for $\bar{n}_s$ in a manner similar to that used by Stockmayer. Funderburk modified the Smith-Ewart recursion relation, however, to permit radical capture by particles to be proportional to the surface area involved. Finally, by ignoring free radical desorption, Funderburk arrived at:

$$\bar{n}_s = \frac{\sigma'}{4} \frac{I_0(\sigma')}{I_1(\sigma')} , \tag{8}$$

where σ' was analogous to σ found in the Stockmayer analysis, and the I's were modified Bessel functions. In the course of evaluating N_T and $\bar{n}_s$ for the system of interest, Funderburk was required to determine the value of the following integral:

$$\int \frac{I_0(x)}{x^{4/5} I_1(x)} dx, \tag{9}$$

when dealing in particle volume coordinates. The variable x, used here as a dummy variable, was Funderburk's dimensionless volume.

In a series of publications (4, 5, 24), DeGraff and Poehlein attempted to predict particle size distributions in a continuous emulsion polymerizer. They coupled the Stockmayer model with the residence time distribution function for a well mixed vessel, thereby relating size distributions to residence time distributions. Their efforts were valiant, but unfortunately untimely in light of Funderburk's analysis. This point was conceded by DeGraff (4).

The works by Stevens and Funderburk and by DeGraff and Poehlein neglected the mechanism of free radical desorption, without explaining

why. However, mathematical analysis shows that to include the desorption of radicals necessitates the evaluation of the integral of a ratio of modified Bessel functions whose orders and arguments are both functions of the integrating variable. By any mathematician's standards such a task would be extremely difficult.

Both investigations also used the Stockmayer model. DeGraff and Poehlein (5) used the model directly, while Stevens and Funderburk (35) used a modified form to account for particle size variations. Neither set of workers justified using batch reactor results in a continuous process analysis, nor did either group justify using an average number of radicals per particle, $\bar{n}_s$, when solving their particle size distribution problem.

A very recent work by Thompson and Stevens (38) showed that the desorption mechanism may be included quite simply in the bimolecular reaction model of Sato and Taniyama (32). This new work permitted particles to have zero or one radical present and distinguished between particles only by the number of radicals present. Particle size variations were not considered. Details of this work are presented later.

RESEARCH PROJECTIONS

The interest in emulsion polymer particle size predictions arises quite naturally, because it is generally accepted that there is some relation between polymer particle size and the molecular weight of the polymer therein. Given such a relation, then, to predict particle size distributions effectively would imply molecular weight predictions, and ultimately the special properties of the product.

With an understanding of what has been done thus far in modelling emulsion polymerization (both batch and continuous) systems, one is in a position to discuss what needs to be done. In light of the many references to free radical desorption in the literature (19, 22, 24, 25, 29, 33, 39, 40), any new model should allow for the possibility of desorption of free radicals from polymer particles. Because of the very nature of the process (continuous flow operation, size dependent radical capture, etc.), there is certain to be a distribution of particle sizes leaving the polymerizer. Any new model, then, should accurately predict particle size variations. Lastly, the averaging process used to determine $\bar{n}$ presented by Stevens and Funderburk (35) and DeGraff and Poehlein (5) is in question. Therefore, any new model should review this point.

This theoretical study will provide a rigorous model for emulsion polymerization which will include the desorption mechanism. The population balance approach will be employed to predict polymer particle size distributions leaving the continuous polymerizer. The determination of $\bar{n}$ will be carried out after the analysis of particle size distributions instead of before said analysis. Lastly, this work will shed new light

on batch emulsion polymerization analysis, and suggest that new equations be studied to that end.

EXTENSION OF SATO-TANIYAMA MODEL

Development

It is desired to mathematically describe the physical system of interest. Figure 1 shows a typical polymerizer where water, monomer, initiator, and emulsifier enter the system. In addition, the reactor shown may not be the first in a series of reactors, thus polymer may be entering the system in question. The same five components may also leave the polymerizer. The mixture is continually stirred to maintain the emulsion.

One of the more interesting and successful attempts at mathematically modelling emulsion polymerization processes was the scheme presented by Sato and Taniyama (31, 32). Their first contribution was to model batch emulsion polymerization, while their second work presented a continuous emulsion polymerization model. The two unique features of their work were that they modelled the polymerization process as if it were a sequence of bimolecular chemical reactions, and, in doing so, they were able to predict effluent concentrations of all the major components present. In short, they developed what might adequately be called a "macroscopic" model for emulsion polymerization. Sato and Taniyama ignored the desorption of free radicals, however.

The efforts to date regarding improvement of this model have been minimal in light of its shortcomings, which are presented later. The goal in this section of the work is to show that the desorption mechanism can easily be included when analyzing continuous stirred tank emulsion polymerization systems. Integrals of complicated Bessel functions need not be evaluated in order to include this simple mechanism. While the

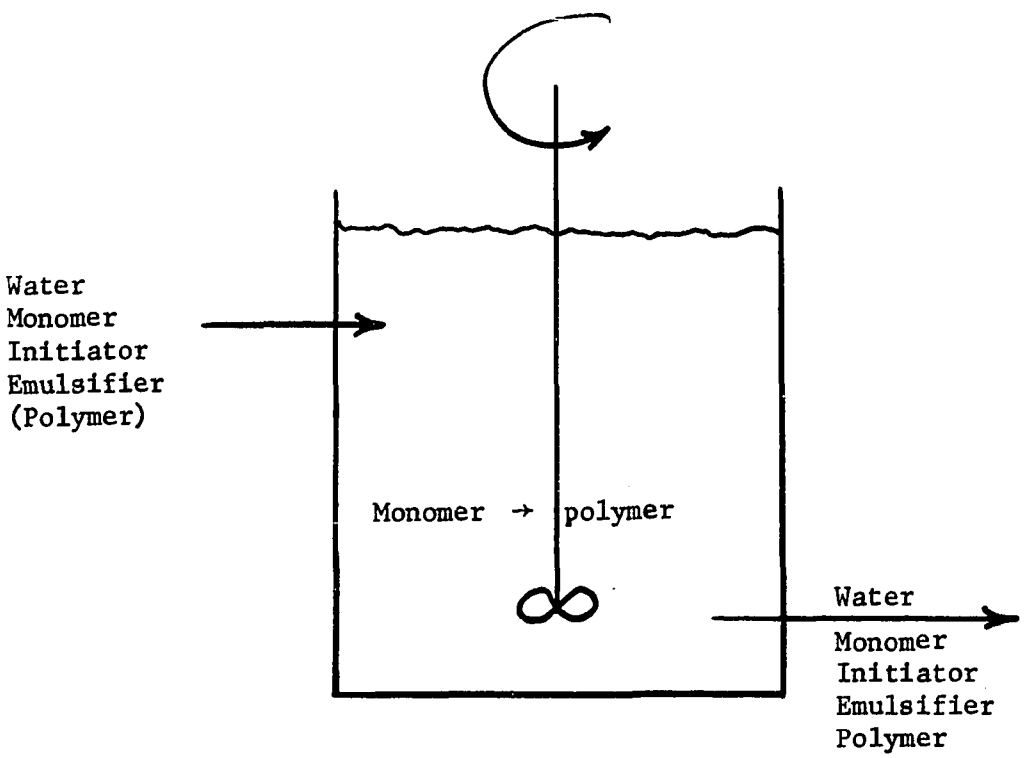

Figure 1. A typical polymerizer arrangement

Sato-Taniyama model including the desorption mechanism is insufficient for providing a detailed description of all mechanistic steps involved, it does show some interesting results. Much of this section is taken directly from an earlier work (38), and is included for completeness.

The essential chemical reactions included in this model may be found in Table 1. To these mechanisms is added the likelihood that a free radical, once inside a polymer particle, may desorb from the particle and reenter the water phase:

$$N_1^* \xrightarrow{k_o} R^* + N_1, \tag{10}$$

where k_o is the specific rate constant describing the magnitude of this effect. Note here that as the desorption mechanism occurs it generates an active free radical in the water phase, which may again attack particles to contribute to growth or termination. This feature of the model is in keeping with the arguments presented by Ugelstad et al. (39). The steady state material balances for the active components involved may now be presented:

$$I_0 - I_1 - k_d \tau F I_1 = 0 \qquad \text{(initiator)} \tag{11}$$

$$M_0 - M_1 - k_p \tau M_m N_1^* = 0 \qquad \text{(monomer)} \tag{12}$$

$$m_0 - m_1 - k_i \tau R^* m_1 - k_v \tau (M_0 - M_1)^{1/3} N^{1/3} N_1^* = 0 \qquad \text{(micelles)} \tag{13}$$

$$-R^* + k_d \tau F I_1 - k_i \tau R^* m_1 - k_i \tau R^* N_1 - k_t \tau R^* N_1^* + \underline{k_o \tau N_1^*} = 0$$

$$\text{(free radicals)} \tag{14}$$

$$-N_1 - k_i \tau R^* N_1 + k_t \tau R^* N_1^* + \underline{k_o \tau N_1^*} = 0 \qquad \text{(dead particles)} \tag{15}$$

$$-N_1^* + k_i \tau R^* m_1 + k_i \tau R^* N_1 - k_t \tau R^* N_1^* - \underline{k_o \tau N_1^*} = 0 \qquad \text{(live particles)} \tag{16}$$

where the underlined terms are the contributions to the material balances due to the desorption of free radicals from the polymer particles. In addition, the total concentration of particles may be represented by:

$$N = N_1 + N_1^*. \tag{17}$$

Table 1. Emulsion polymerization reaction expressions

decomposition of initiator	$I \longrightarrow R^*$
initiation	$R^* + M \longrightarrow N_1^*$
growth	$N_1^* + M \longrightarrow N_1^*$
termination	$R^* + N_1^* \longrightarrow N_1$
re-initiation	$R^* + N_1 \longrightarrow N_1^*$

Equations (11) - (17) were solved simultaneously to describe the steady state behavior of the polymer system. The mathematical description of the dependent variables (I_1, M_1, m_1, R^*, N_1, N_1^*, and N) as functions of the independent parameters (I_0, S_0, τ, etc.) should give some prediction of the behavior of the effluent stream leaving the reactor.

The last term in Equation (13) involves a constant, k_v. This term describes the loss of micelles to coat the polymer particle surfaces, a coating which is assumed to be monolayer in nature. The development of the constant k_v is presented in the literature (20, 31, 32), and is:

$$k_v = \frac{3.22 k_p M_m N_A^{1/3}}{a_s S_9} (M_w V_p)^{2/3} \left\{ 1 - \frac{M_w M_m V_m}{1000} \right\}^{-2/3}, \tag{18}$$

where:

a_s = surface area covered by soap molecules

k_p = polymerization rate constant

M_m = concentration of monomer in particles

M_w = molecular weight of monomer

S_9 = number of molecules per micelle

V_m = specific volume of monomer

V_p = specific volume of polymer

The constant k_v is observed to depend on the properties of the monomer used, the polymer produced, and the emulsifier molecules in the system.

Numerical Results

The set of simultaneous Equations (11) - (17) were solved in the manner described in Appendix A. Numerical values of the constants used in these solutions are listed in Table 2. These numbers, taken essentially from the work by Sato and Taniyama (31, 32), were used to generate Figures 2 - 6.

The total concentration of particles, N, is shown to depend on the initiator concentration in the feed, I_0, and the desorption parameter, k_0, in Figure 2. For small values of I_0, the curves of different k_0 form parallel lines having slopes (on a log-log scale) of about 1.0. For large I_0, the curves converge to a single limiting curve, becoming independent of I_0. For comparison, the curve having $k_0 = 0$, and for $I_0 > 10^{-4}$ gm mole/liter, corresponds to Figure 1 given by Sato and Taniyama (32). It is interesting to notice that higher values of the desorption parameter

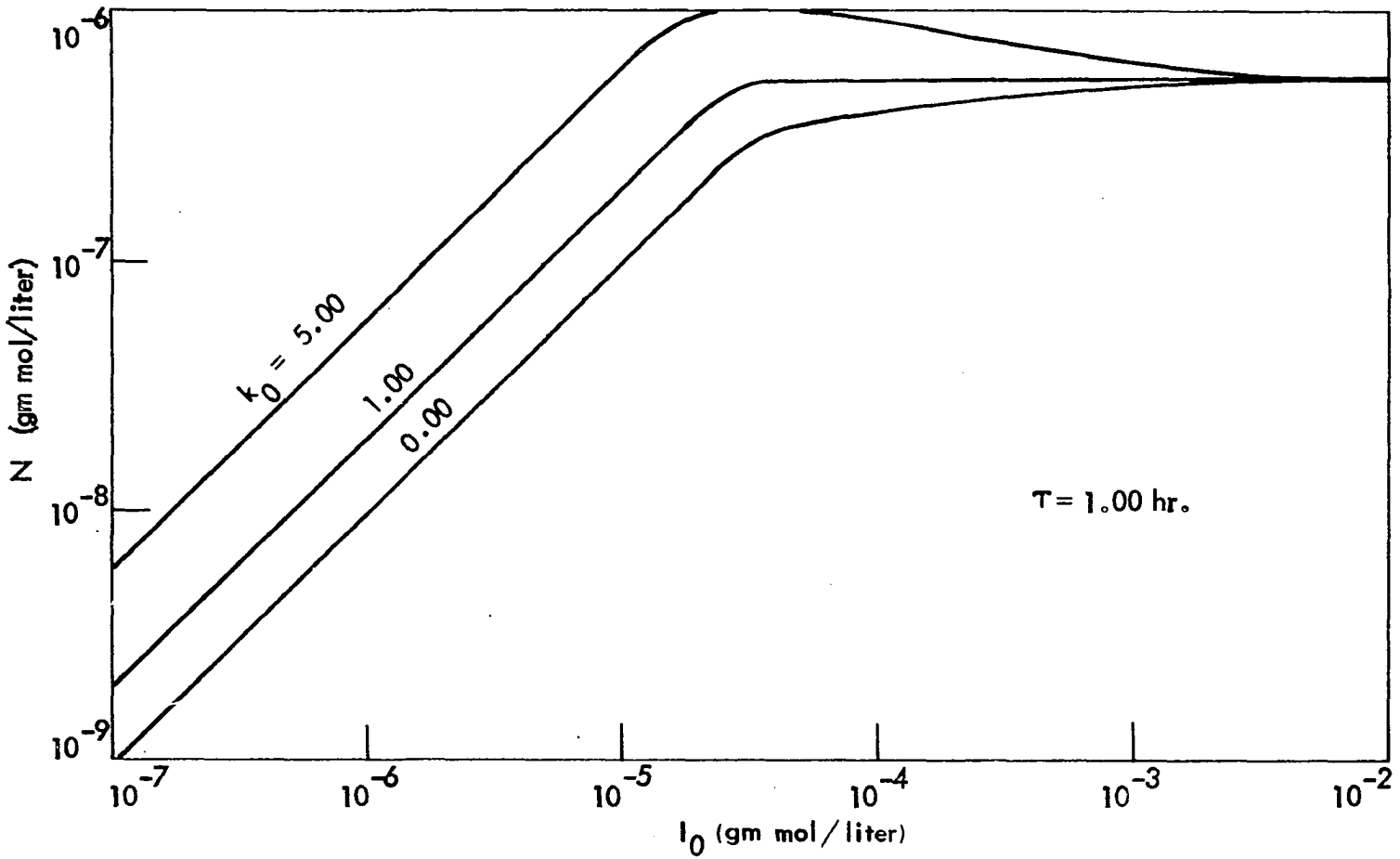

Figure 2. Total concentration of particles as a function of initiator feed concentration

Table 2 Values of rate constants and physical properties used for Figures (2) - (8)

F	1.00
k_d	10^{-2} 1/hr
$k_i = k_t$	10^{-6} liter/gm mole hr
k_p	5×10^5 liter part./gm mole hr
k_v	1.63×10^5 liter/gm mole hr
M_0	3.5 gm mole/liter
M_m	5.0 gm mole/liter
S_0	10^{-2} gm mole/liter
S_9	25

lead to larger concentrations of polymer particles generated in the reactor system. This result stems from the fact that the desorption mechanism tends to maintain a higher free radical concentration in the water phase, increasing the possibility a micelle will be stung by a radical. Comparison of experimental data to such theoretical curves should give one estimate of the value of k_o.

The term $\bar{n}_s$ represents the average distribution of free radicals in polymer particles, i.e. the fraction of polymer particles growing at any time. Mathematically, $\bar{n}_s$ was found from:

$$\bar{n}_s = N_1^*/N. \tag{19}$$

Such a quantity is relevant simply because it indicates the degree to

which polymerization is occurring in the steady state system. The dependence of $\bar{n}_s$ on I_0 and k_o is shown in Figure 3. At low values of I_0, the higher the parameter k_o the lower the value of $\bar{n}_s$; there is no variation of $\bar{n}_s$ with I_0. At high values of I_0, the curves converge to a single value of $\bar{n}_s = 0.5$.

At low values of I_0 the free radicals generated in solution reside in the particles, because absorption of these is fast relative to their generation. As desorption becomes more significant, more and more of these absorbed radicals are shoved back into the water phase, thus shifting the free radical distribution (i.e. lowering $\bar{n}_s$). At high I_0 values the system is flooded with free radicals, generated from initiator molecules, to the extent that the contribution of free radicals from the desorption mechanism is insignificant. The only meaningful mechanistic steps in that case are absorption and termination of radicals.

A second reason for the interest in $\bar{n}_s$ arises out of a desire to know the absolute rate of polymerization in the reactor, as given by:

$$R_p = \frac{k_p M_m N}{N_A} \bar{n}_s . \qquad (20)$$

Figure 4 shows how the rate of polymerization varies with I_0 and k_o. While R_p depends on both N and $\bar{n}_s$ it would be difficult to distinguish a meaningful value of k_o from experimental results of R_p vs. I_0. Scatter in the experimental data would make determination of k_o for the system impossible. Figures 2 - 4, however, suggest that if R_p and N could be measured independently at sufficiently low values of I_0, $\bar{n}_s$ may be

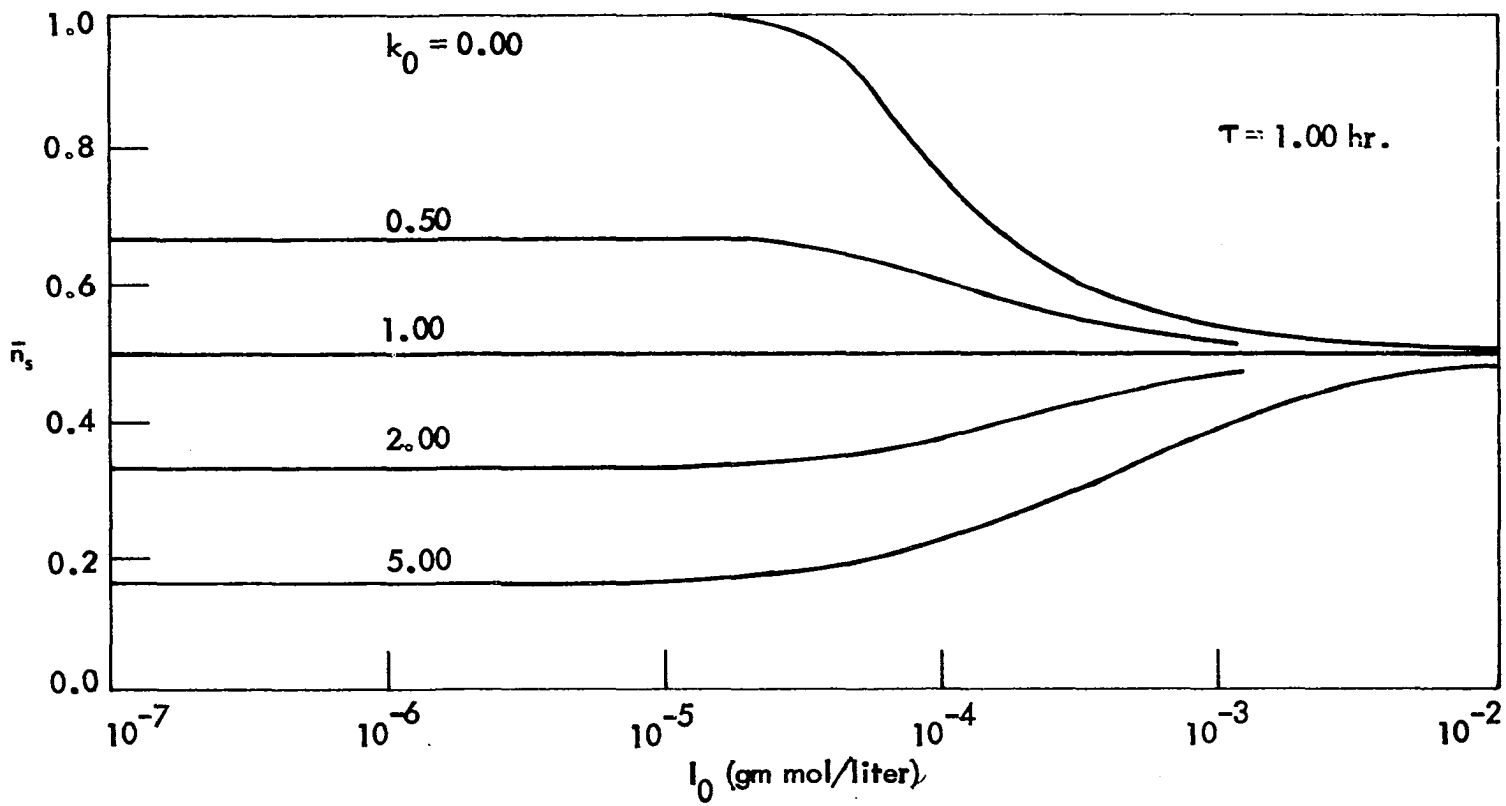

Figure 3. Dependence of $\bar{n}_s$ on I_0 and k_0

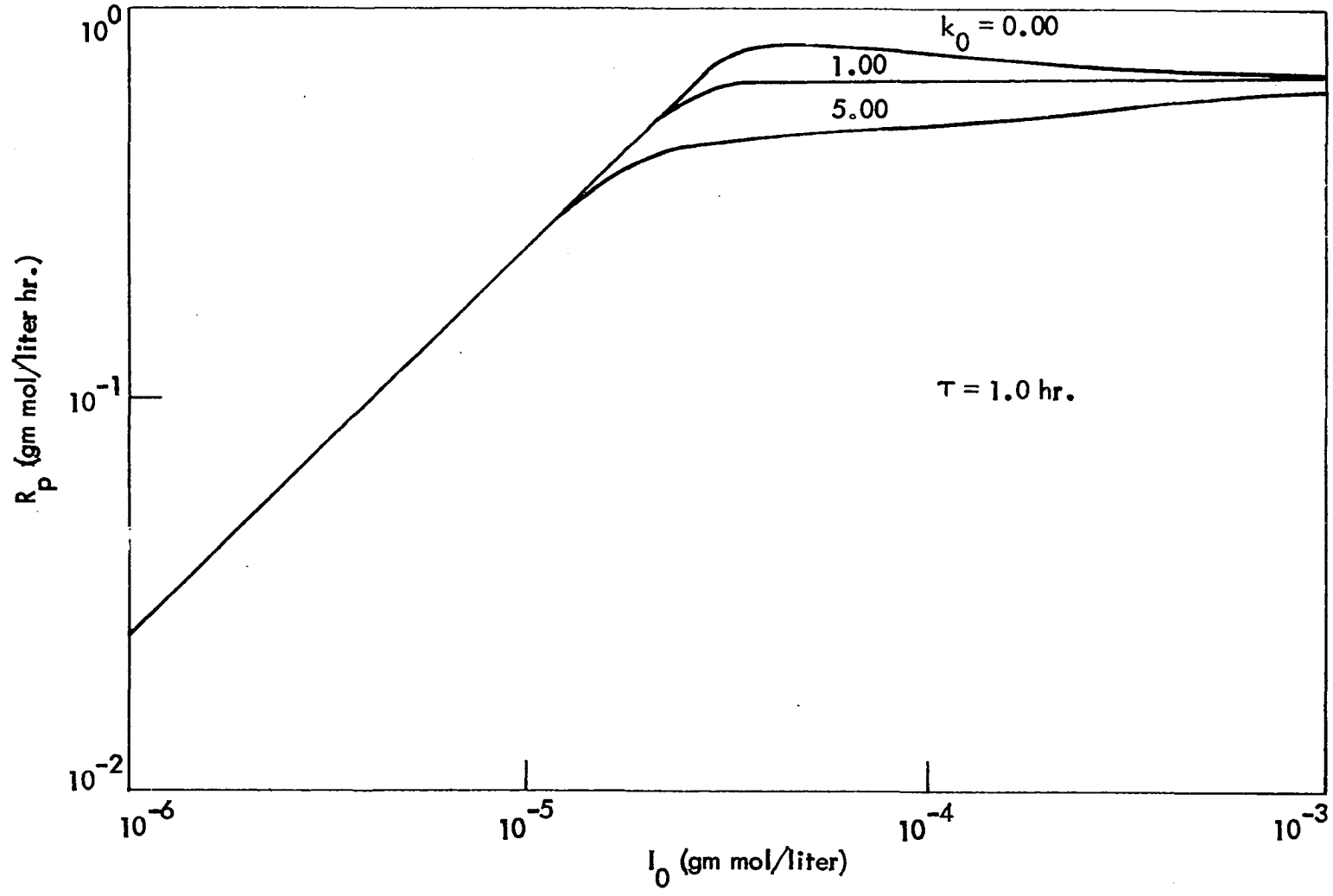

Figure 4. Dependence of rate of polymerization on I_0 and k_0

determined from Equation (20). A reliable value of k_o could be found in such a way, providing a second means for estimating a value of k_o.

Figures 5 & 6 show the dependence of the total number of particles, N, on the residence time, τ, and the parameter k_o. The trend observed is that there is an optimum value of τ which will yield a maximum number of particles. This effect has been observed elsewhere (4, 20). For any value of τ the number of particles increases as k_o increases. This observation is reasonable and is in keeping with the results previously discussed.

Analysis of DeGraff's Data

Some data for the polymerization of styrene at 70^0C was extracted from the literature to test this macroscopic model (4). Ammonium persulfate was used as the initiator; sodium lauryl sulfate was the emulsifier. The physical data used to generate theoretical curves for Figures 7 & 8 are listed in Table 3. All other pertinent data are given on the respective figures.

The quantity $k_d \tau F I_1$ in Equation (14) represents the formation of free radicals by decomposition of initiator molecules. This term was multiplied by a factor of two when analyzing DeGraff's data as his initiator decomposed to give two free radicals.

In Figure 7 is shown experimental data of the total number of particles at varying levels of initiator concentration in the feed stream. The theoretical curves from the current work are shown for values of $k_o = 0$ and $k_o = 5$, along with the theoretical predictions of DeGraff (4).

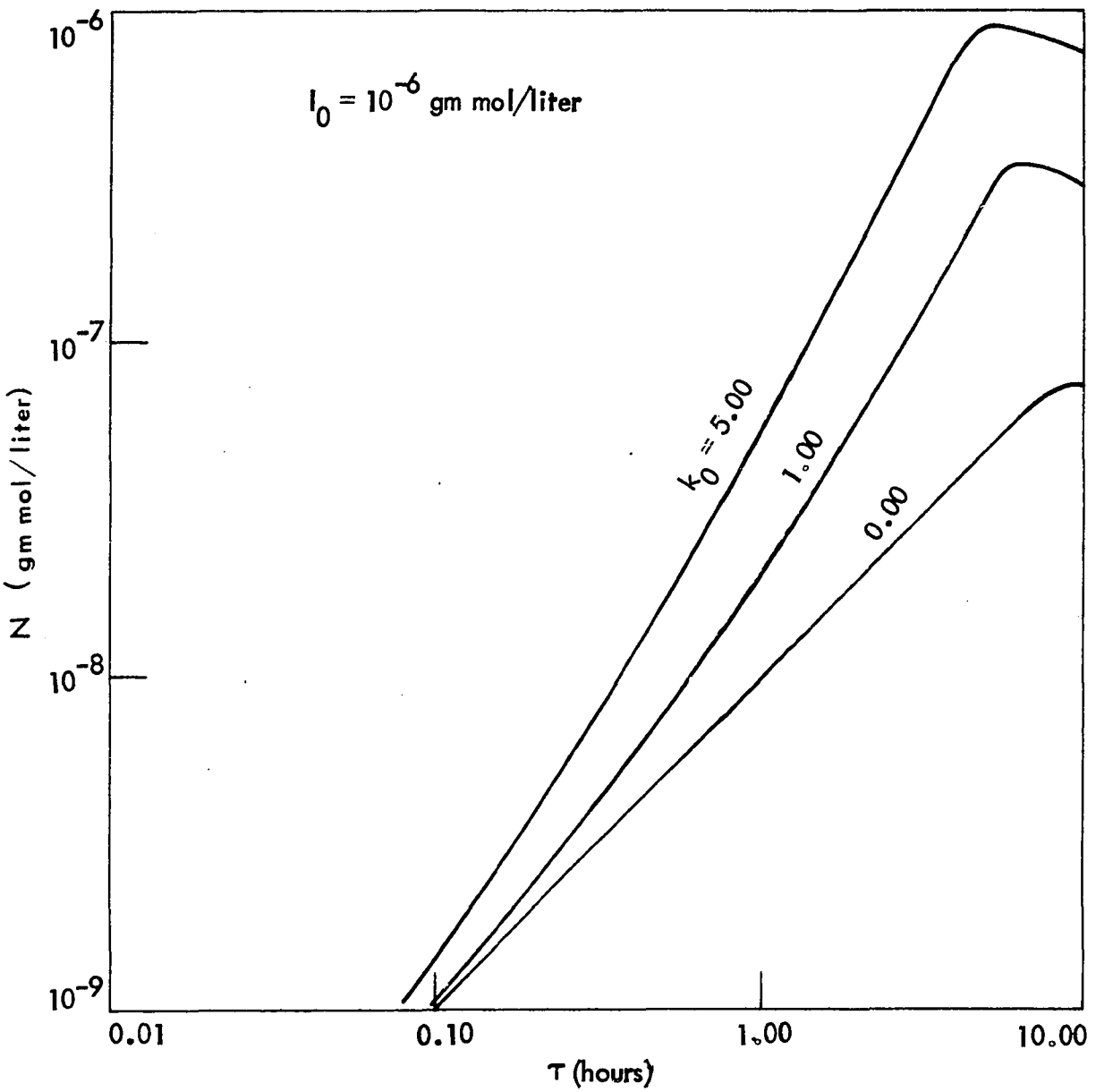

Figure 5. Total number of particles as a function of residence time

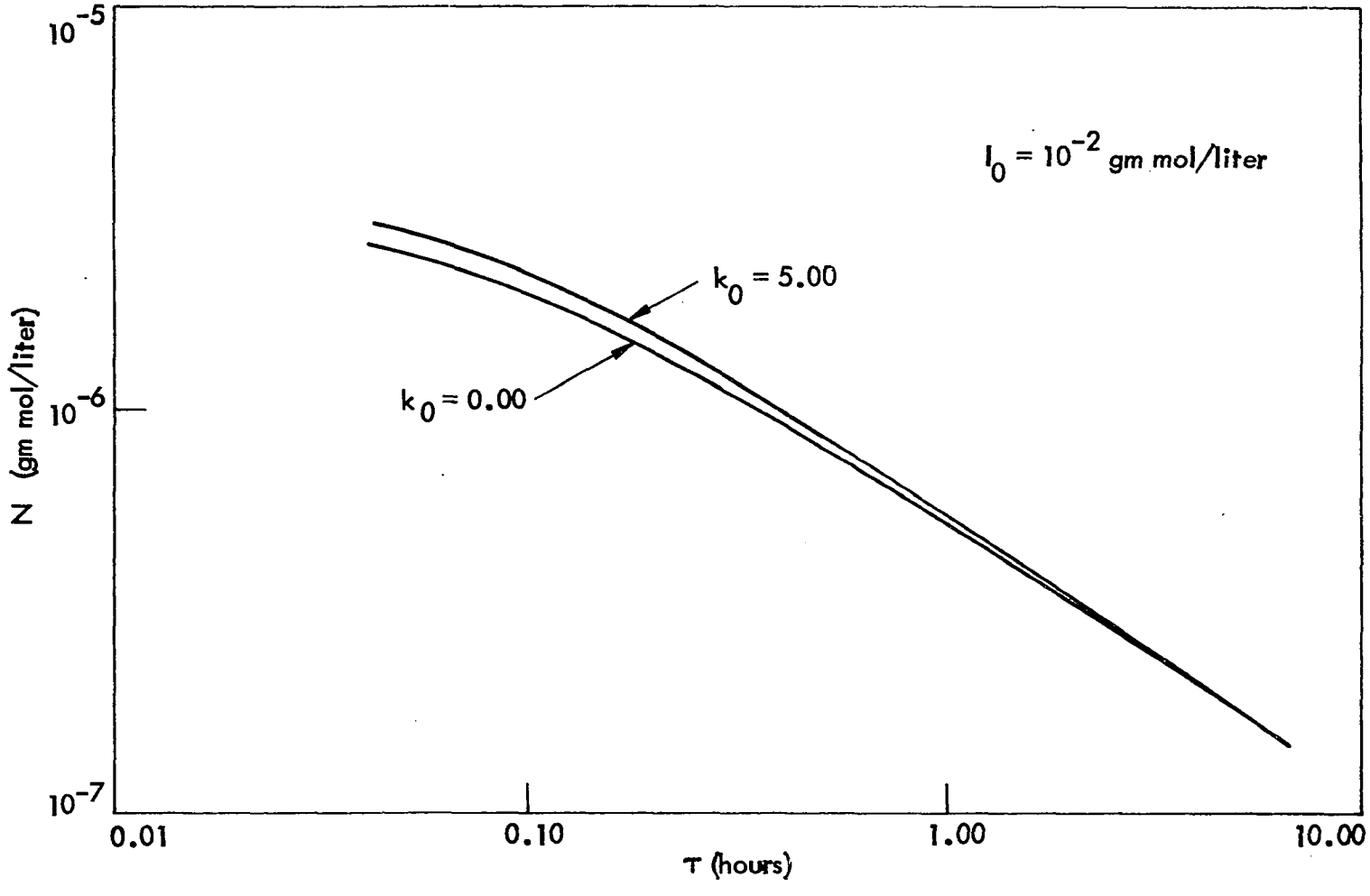

Figure 6. Total number of particles as a function of residence time

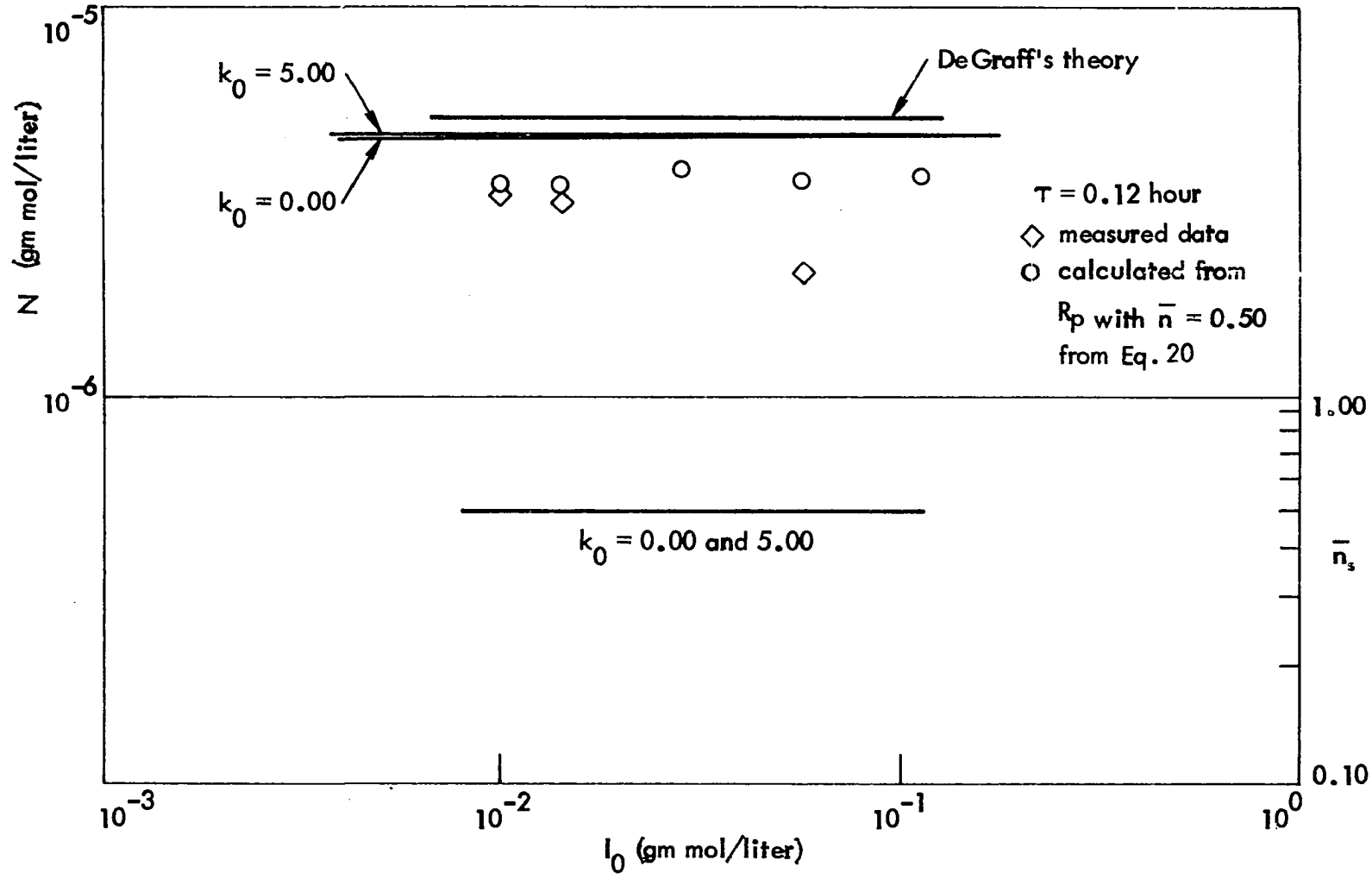

Figure 7. Comparison of macroscopic model to DeGraff's data (4)

Table 3. Values used in analysis of DeGraff's data (4)

F	1.00
k_d	8.388×10^{-2} 1/hr
$k_i = k_t$	2.592×10^{10} liter/gm mole hr
k_p	9.54×10^{5} liter part./gm mole hr
k_v	1.49×10^{5} liter/gm mole
M_0	3.055 gm mole/liter
M_m	5.2 gm mole/liter
S_0	0.0628 gm mole/liter
S_9	100

Corresponding values of $\bar{n}_s$ calculated from this work are plotted on the same graph.

Figure 8 shows how the total number of particles, N, varies with the residence time, τ. The data are from the work by DeGraff (4). Once again his model predictions and the predictions from the current work are shown. Predicted values of $\bar{n}_s$ from this work are shown.

The current model describes the data as well as, if not better than, DeGraff's model. Unfortunately, his model suffers from the need to evaluate integrals of ratios of modified Bessel functions, much like the integrals described in Equation (9). As a result he cannot hope to include the desorption of free radicals in his model. In addition, because $\bar{n}_s$ is so very nearly equal to 0.5 in all his data, he never really tested the validity of his model.

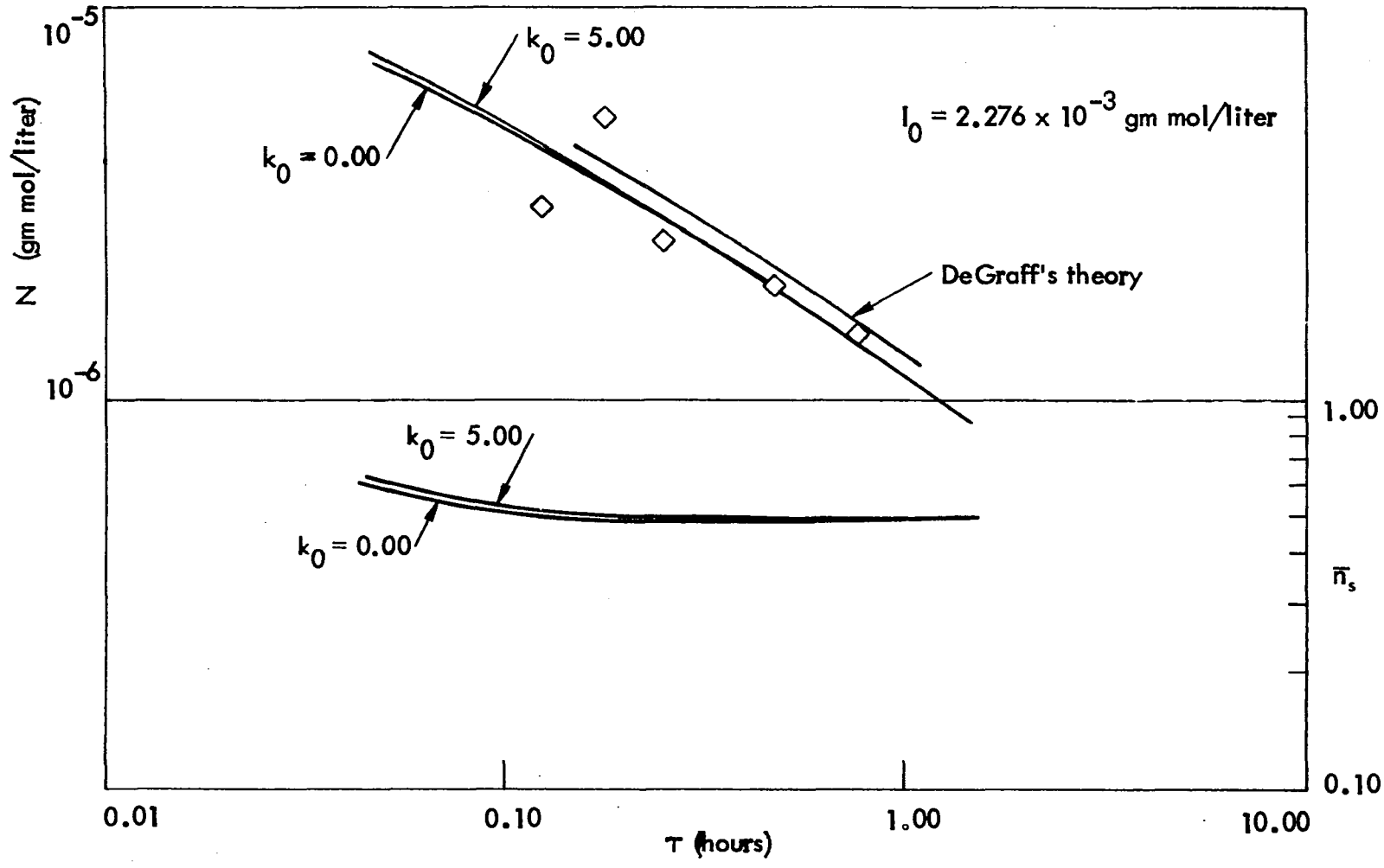

Figure 8. Comparison of macroscopic model to DeGraff's data (4)

Limitations

While the current model describes DeGraff's data reasonably well, there are rather obvious inherent shortcomings which should not be forgotten or considered lightly. In addition, the assumptions used in developing this model should be reviewed.

The current work employed certain assumptions regarding the reactor system itself. Steady state was assumed; no transients were considered. The stirred tank was assumed well mixed, and it was assumed the effluent stream was of the same composition in all components as the reactor itself. There was no input of polymer particles to the reactor, i.e. the analysis would be valid for only the first in a series of polymer reactors. The model is sufficiently general to include polymer in the feed stream.

In the reactor the particles developed were assumed to be spherical in shape. This assumption was used in the derivation of k_v.

The monomer level in the particles, M_m, was assumed to be constant.

It was assumed that the desorption of radicals occurred from polymer particles only. Micelles did not give up their radicals.

It was assumed that all particles were chemically active to the same degree. Micelles or polymer particles were equally likely to be stung by radicals. This assumption resulted from not considering size variations among the particles.

Polymer particles were allowed to house one radical at most. The arrival of a second radical resulted in immediate termination of the two. By letting $k_i = k_t$, one is really saying that both live and dead particles

capture free radicals at the same rate (The terms k_i and k_t are really misnomers in this context.).

Lastly, chain transfer was not considered at this point. This effect was considered of secondary importance.

In view of the severe limitations inherent in this model, one must not stop here, but proceed to more relevant analyses of emulsion polymerization systems.

DEVELOPMENT OF POPULATION BALANCE MODEL

Introductory Remarks

In this section a new model will be developed to further investigate the emulsion polymer system shown in Figure 1.

In any perfectly mixed vessel with feed and effluent streams there will be a distribution of residence times of the material in that vessel. This physical phenomenon, plus the nature of the polymerization process, will give rise to a distribution of sizes of polymer particles leaving the reactor. It is the goal of this study to be able to effectively predict this distribution. To do this, the population balance approach, discussed in the literature (7, 26, 27, 35), will be employed. A statistical mechanical technique could have been used (17). Both techniques lead to the same result; the choice of mathematical approaches was rather arbitrary.

It is convenient to define a number density of particles, N_n, which contains n free radicals. This quantity is a function of both internal (characteristic of the particle dimensions) and external (characteristic of the system coordinates) variables:

$$N_n = N_n(x_1, x_2, x_3, v, t), \tag{21}$$

where n is a parameter. The variable n could have been considered an internal variable, however, it is a discrete variable, and this fact would have caused trouble later. Note that to describe the polymer particle size distribution completely will require that a collection of quantities (N_0, N_1, N_2,...) be described as functions of the internal and

external variables. Note also that by the definition of N_n, the quantity $N_n dv$ represents the concentration of particles in the differential size range v to v + dv containing n free radicals. While in theory the N_n functions could be considered to vary with position in the reactor vessel, it will be more fruitful to assume the vessel is uniformly mixed. The N_n functions would then be given by:

$$N_n = N_n(v, t). \tag{22}$$

General Numbers Balance

The expression representing a population balance for the N_n-type particle can now be formulated. Written in general terms it is:

$$V\frac{d}{dt}\int_{v_1}^{v_2} N_n\, dv = \int_{v_1}^{v_2} (qN_{n_i} - qN_n)dv + V\int_{v_1}^{v_2} r_{N_n}\, dv, \tag{23}$$

where r_{N_n} represents the net rate of formation of the N_n-type particle per unit of system volume. The four terms in Equation 23 represent accumulation of particles, input of particles, outflow of particles, and generation of particles in the system, respectively. The balance is made on all particles in the size range v_1 to v_2 having n active free radicals. In Equation 23 it has been assumed that the size range v_1 to v_2 is purely arbitrary, and that the volumetric flow rate through the system is constant. It was also implicitly assumed that the composition in the effluent stream is identical to the composition in the reactor. This assumption is not so easily justified or accommodated as in the case of single phase mixtures. Classified withdrawal, as discussed by Stevens

and Davitt (34), can frequently be a problem and particulate systems must be designed with this thought in mind. Lastly, the system volume was assumed to be fixed. Equation 23 is analogous to a material balance, except that the balance is made on particle numbers instead of polymer mass.

Equation 23 may be rearranged to yield the following expression:

$$\frac{d}{dt}\int_{v_1}^{v_2} N_n dv = \int_{v_1}^{v_2} \frac{N_{n_i} - N_n}{\tau} dv + \int_{v_1}^{v_2} r_{N_n} dv \ . \tag{24}$$

By using Leibnitz's rule for differentiation of an integral on the left hand side, one concludes that:

$$\int_{v_1}^{v_2} \left\{ \frac{\partial N_n}{\partial t} + \frac{\partial}{\partial v}(N_n R_{v_n}) \right\} dv = \int_{v_1}^{v_2} \frac{N_{n_i} - N_n}{\tau} dv + \int_{v_1}^{v_2} r_{N_n} dv, \tag{25}$$

where the following definition has been introduced:

$$R_{v_n} \equiv \frac{dv}{dt} \ . \tag{26}$$

R_{v_n} expresses the volumetric growth rate of the N_n-type particle. Finally, by rearranging Equation 25, one has:

$$\int_{v_1}^{v_2} \left\{ \frac{\partial N_n}{\partial t} + \frac{\partial}{\partial v}(N_n R_{v_n}) - \frac{N_{n_i} - N_n}{\tau} - r_{N_n} \right\} dv = 0. \tag{27}$$

Because the size range was chosen arbitrarily, if the integral in Equation 27 is identically zero, then the integrand itself must be identically zero, and:

$$\frac{\partial N_n}{\partial t} + \frac{\partial}{\partial v}(N_n R_{v_n}) = \frac{N_{n_i} - N_n}{\tau} + r_{N_n} \tag{28}$$

To this point few assumptions have been made. Both the flow rate, q, and the system volume, V, were assumed constant, implying constant τ in Equation 28. It was also assumed that the system was homogeneously mixed, i.e. samples taken from various locations in the tank would be the same. Implicit in the derivation was the assumption that the effluent stream was of the same composition as the contents of the tank. Other than these few assumptions, Equation 28 is perfectly general. It is left only to arrive at meaningful expressions for R_{v_n} and r_{N_n} to solve the system of equations for the N_n-type particles.

Observe the generality of Equation 28. This equation, with the appropriate boundary conditions, should describe the behavior of a transient continuous emulsion polymerizer. With the time derivative set equal to zero, a steady state continuous emulsion polymerizer is implied. An infinite residence time (q=0) yields an equation describing the operation of a batch reactor. A plug flow reactor is described by the same equation as the batch reactor when the real time variable, t, is changed to a space time, s. These special cases are shown in Table 4. Equation 28 should describe the particle size distribution in either emulsion or suspension polymerization, where one or more monomers (mono- or co-polymerization) are present. The only remaining task is to describe the volumetric growth rate, R_{v_n}, and the rate of particle-type formation, r_{N_n}, for the particular system of interest.

Table 4. Model variations

Reactor Systems	Applicable Equations
transient continuous polymerizer	$\frac{\partial N_n}{\partial t} + \frac{\partial}{\partial v}(N_n R_{v_n}) = \frac{N_{n_i} - N_n}{\tau} + r_{N_n}$
steady state continuous polymerizer	$\frac{d}{dv}(N_n R_{v_n}) = \frac{N_{n_i} - N_n}{\tau} + r_{N_n}$
batch emulsion polymerizer	$\frac{\partial N_n}{\partial t} + \frac{\partial}{\partial v}(N_n R_{v_n}) = r_{N_n}$
steady state plug flow polymerizer	$\frac{\partial N_n}{\partial s} + \frac{\partial}{\partial v}(N_n R_{v_n}) = r_{N_n}$

Emulsion Polymerization Rate Expression

The first step toward solving Equation 28 is to specify a rate of formation for the N_n-type particle in an emulsion polymerization system. It turns out that this expression was given in the literature by Smith and Ewart (33). The recursion relation which they presented is actually a rate of formation expression, r_{N_n}, for the N_n-type particle. Their expression cannot be used directly here, however, because their quantity N_n represented a concentration of particles, while herein the term $N_n dv$ represents a concentration of particles. Smith and Ewart assumed all particles were the same size, while this study presupposes a particle size distribution. This discrepancy poses no problem, however, because the polymer particles should be formed in a similar fashion whether one assumes uniform particle sizes or a particle size distribution. Funderburk (7) showed that the Smith-Ewart model could be modified to account for particle size variation. Whereas Funderburk proceeded to average the recursion relation in a manner similar to Stockmayer's technique, the procedure here will be to use this relation directly in Equation 28. The rate of formation of the N_n-type particle can be written as:

$$r_{N_n} = \frac{k_t}{N_A v}\left\{(n+2)(n+1)N_{n+2} - n(n-1)N_n\right\}$$
$$+ \frac{(4\pi)^{1/3}(3)^{2/3}\rho_A v^{2/3}}{S}\left\{N_{n-1} - N_n\right\} \qquad (29)$$
$$+ \frac{(4\pi)^{1/3}(3)^{2/3}k_o}{v^{1/3}}\left\{(n+1)N_{n+1} - nN_n\right\}$$

where the numerical coefficients arise as a result of expressing particle surface area in terms of its volume. Spherical particles have been

assumed. Note that the mechanism of absorption of free radicals has been altered to be proportional to the fraction of the surface area involved. Discussion of this point may be found elsewhere (7, 10). Unlike in Funderburk's work, the desorption mechanism may be included here with no difficulty.

The terms in Equation 29 represent actual mechanisms occurring in the reaction. The first term is the contribution from radical termination in a particle; the second term describes radical absorption by particles; the last term illustrates the effect of free radical desorption. Note that each mechanistic step contains a positive and a negative contribution. Also notice that each mechanism is in some way affected by the volume of the polymer particle.

Equation 29 may be compacted slightly by the introduction of new constants:

$$\alpha = \frac{k_t}{N_A}, \quad \beta = \frac{(4\pi)^{1/3}(3)^{2/3}\rho_A}{S}, \text{ and } \gamma = (4\pi)^{1/3}(3)^{2/3}k_o. \tag{30}$$

Equation 29 is now written as:

$$r_{N_n} = \frac{\alpha}{v}\left\{(n+2)(n+1)N_{n+2} - n(n-1)N_n\right\}$$

$$+ \beta v^{2/3}\left\{N_{n-1} - N_n\right\} \tag{31}$$

$$+ \frac{\gamma}{v^{1/3}}\left\{(n+1)N_{n+1} - nN_n\right\}$$

Equation 31 is the final form which will be used later in Equation 28.

Particle Growth Rate

Attention must next be focused on the particle growth rate term, R_{v_n}. Once again this quantity is available from the literature. Gardon (9) implicitly stated that the particle growth rate was proportional to the free radical content. O'Toole (23) stated this directly. Gardon presented the proportionality constant. The following expression for R_{v_n} will be used in Equation 28 to describe emulsion polymer particle growth:

$$R_{v_n} \equiv \frac{dv}{dt} = Kn, \tag{32}$$

where the constant K is defined as:

$$K \equiv k_p \frac{\rho_m \phi_m}{N_A \rho_p (1-\phi_m)} . \tag{33}$$

The model for emulsion polymerization is now ready to be assembled and investigated.

Complete Assembled Model

By combining Equations 28, 31, and 32, the complete model for emulsion polymerization is realized:

$$\frac{\partial N_n}{\partial t} + \frac{\partial}{\partial v}(N_n R_{v_n}) = \frac{N_{n_i} - N_n}{\tau} + \frac{\alpha}{v}\left\{(n+2)(n+1)N_{n+2} - n(n-1)N_n\right\}$$
$$+ \beta v^{2/3}\left\{N_{n-1} - N_n\right\} \tag{34}$$
$$+ \frac{\gamma}{v^{1/3}}\left\{(n+1)N_{n+1} - nN_n\right\} ,$$

where it is understood that a N_n function having a negative subscript is non-existent and set identically equal to zero. The solution of this system of equations (remember that n is a parameter), with the appropriate boundary conditions and the appropriate terms discarded (if any), should describe the behavior of an emulsion polymerizer.

Only two assumptions have been made in addition to those made in deriving Equation 28. First, the particle growth rate was assumed to be proportional to the number of free radicals present in a particle. Second, the particles were assumed spherical in shape in order to relate surface area to particle volume.

Writing down the first few equations generated by Equation 34 gives:

$$\frac{\partial N_0}{\partial t} = \frac{N_{0i} - N_0}{\tau} + \frac{\alpha}{v}(2N_2) - \beta v^{2/3}(N_0) + \frac{\gamma}{v^{1/3}}(N_1) \tag{35}$$

$$\frac{\partial N_1}{\partial t} + \frac{\partial}{\partial v}(KN_1) = \frac{N_{1_i} - N_1}{\tau} + \frac{\alpha}{v}(6N_3) + \beta v^{2/3}(N_0 - N_1)$$

$$+ \frac{\gamma}{v^{1/3}}(2N_2 - N_1) \tag{36}$$

$$\frac{\partial N_2}{\partial t} + \frac{\partial}{\partial v}(2KN_2) = \frac{N_{2i} - N_2}{\tau} + \frac{\alpha}{v}(12N_4 - 2N_2) + \beta v^{2/3}(N_1 - N_2)$$

$$+ \frac{\gamma}{v^{1/3}}(3N_3 - 2N_2) \tag{37}$$

In the above equations the parameter n has taken on the values of n = 0, 1, and 2.

In order to solve the continuous or the batch emulsion polymer

problem an appropriate set of boundary conditions must be specified. In particular, the number density of particles at "zero volume" containing n = 1, 2, 3,... free radicals must be known. The term "zero volume" will henceforth be taken to mean the smallest possible size of a polymer particle, or micellar volume. The zero volume boundary condition for the N_0 function is not required, as this type of particle is never in a growing state, and the equation describing the N_0 function is merely algebraic. For the particles where n>1, it may be safely assumed that N_n at zero volume is zero; a particle at zero volume cannot contain more than one free radical. The only boundary condition required is the number density at zero volume of the N_1-type particles. This boundary condition will be developed later for the steady state continuous emulsion polymerizer.

RESULTS OF CSTR ANALYSIS

Introduction and Dimensionless Form

The bulk of the remainder of this text will be devoted to an in depth study of the description of the steady state continuous stirred tank polymerizer. At the outset it is fruitful to consider the steady state population balance generated from Equation 34 and make the equation dimensionless, resulting in:

$$\frac{d}{d\zeta}(nX_n) = -A5X_n + \frac{A7}{\zeta}\left\{(n+2)(n+1)X_{n+2} - n(n-1)X_n\right\}$$

$$+ A4\zeta^{2/3}\left\{X_{n-1} - X_n\right\} + \frac{A6}{\zeta^{1/3}}\left\{(n+1)X_{n+1} - nX_n\right\}, \quad (38)$$

where the following definitions have been employed:

$\zeta = v/v_0$, $\quad A4 = \beta v_0^{5/3}/K$, $\quad A6 = \gamma v_0^{2/3}/K$,

$X_n = N_n/N_{T_0}$, $\quad A5 = v_0/K\tau$, and $\quad A7 = \alpha/K$.

Note that the problem is now reduced to a system of equations containing four adjustable dimensionless parameters, the parameters representing the four primary mechanisms occurring in the polymer system: A4 represents the absorption of free radicals, A5 represents bulk flow in the system, A6 incorporates the desorption mechanism, and A7 expresses the rate of mutual termination of free radicals. Particle growth is present in each constant. In reality, these four parameters represent the ratio of the magnitudes of the four mechanisms to the particle growth rate constant. More explicit representation of these four dimensionless constants is shown in Appendix B.

Observe that in Equation 38 it has been assumed that there is no polymer in the feed. That is, the following analysis would be valid for the first polymerizer in a series, or a single stirred tank polymerizer.

Notes on the Boundary Condition

Before setting out to solve the steady state population balance relations for any number of particle types it is advantageous to examine the characteristics of a very simplified case. As it turns out, the solution to this problem will become important later.

Assume throughout this section that only the X_0- and X_1-type particles exist. That is, a particle may house only one radical at a time, instantaneous termination occurring upon the arrival of a second free radical. The goal of mathematical analysis would then be to generate information about the dependence of the X_0 and X_1 functions on the parameters involved in the system.

From Equation 38, when n = 0, the algebraic expression for X_0 arises:

$$0 = - A5X_0 + A4\zeta^{2/3}(-X_0) + \frac{A6}{\zeta^{1/3}}(X_1), \tag{39}$$

where the value of all X_n's for n>1 have been set equal to zero. The above relation is not quite correct, however, because the assumption has been made that termination of two radicals is limited only by the arrival of a second radical. The result of this truncation assumption is the corrected equation below:

$$0 = - A5X_0 + A4\zeta^{2/3}(X_1-X_0) + \frac{A6}{\zeta^{1/3}}(X_1). \tag{40}$$

That is, the arrival of a free radical to an X_1-type particle immediately gives rise to an X_0-type particle.

One could now write down the population balance relation for the X_1-type particle by allowing n to take on the value of one in equation 38. This differential equation could then be solved with Equation 40 to yield particle size distribution information. Alternatively, one can obtain less information from an easier solution by settling for only information at the size of the particle nuclei, $\zeta = 1$. Under such a constraint, a second applicable algebraic relation is:

$$X_0 + X_1 = 1.0. \tag{41}$$

This condition will eventually supply the boundary condition for further work.

Allowing ζ to take on the value of 1.0 in Equation (40) yields:

$$0 = - A5X_0 + A4(X_1-X_0) + A6(X_1), \tag{42}$$

or:

$$0 = - X_0 + A3(X_1-X_0) + A1(X_1), \tag{43}$$

where:

$$A1 = A6/A5 \quad \text{and} \quad A3 = A4/A5.$$

Solving Equations (41) and (43) together, one arrives at:

$$X_0 = \frac{A1 + A3}{1 + A1 + 2A3},$$

$$X_1 = \frac{1 + A3}{1 + A1 + 2A3}, \text{ and} \tag{44}$$

$$\bar{n} = \frac{X_1}{X_0 + X_1} = X_1.$$

Recall now that A4 is proportional to the initiator feed concentration, while A1 is the measure of the desorption mechanism. Figure 9 illustrates the dependence of $\bar{n}$ on A4, where A1 is an adjustable parameter. Note the similarity to Figure 3. All qualitative comments made for Figure 3 now also apply to Figure 9. The choice of A5 was dictated by DeGraff's work (4).

Equations (44), shown in Figure 9, now form the boundary conditions (at $\zeta = 1$) for the solution of the full assembled problem.

Discussion of Solution Technique and the Computer Program

The population balance equations previously developed were solved on the computers (IBM 360-model 65 and IBM 370-model 158) at Iowa State University employing a fourth-order Runge-Kutta scheme. The numerical integration was carried out in double precision along the dimensionless volume axis, ζ. A listing of the program is shown in Appendix D.

Several independent parameters were varied in the course of this work to note their effect on the particle size distribution results. Figure 10 shows the values of the parameters used in these studies. The parameter values of the base case are outlined there also.

The computer program accepts information read in regarding the values of the four independent parameters. After some initialization, the first set of values of the various number density functions are calculated using the boundary condition equations derived on pages 47 - 49.

The first integration step is performed using a modified routine, modified to hold the value of X_0 fixed during this first step. This

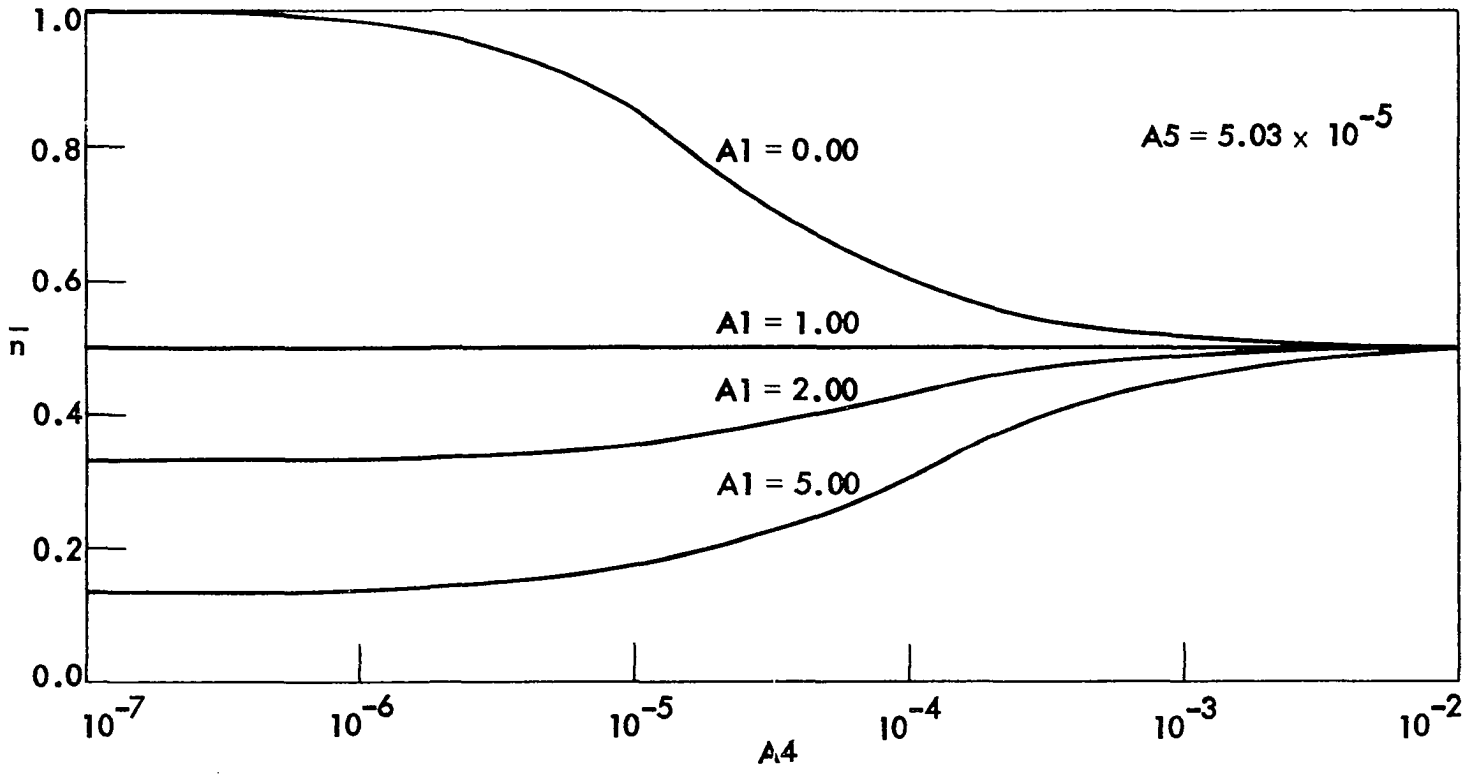

Figure 9. Dependence of $\bar{n}$ on A4 and A1 from population balance model ($X_n = 0$ for $n > 1$)

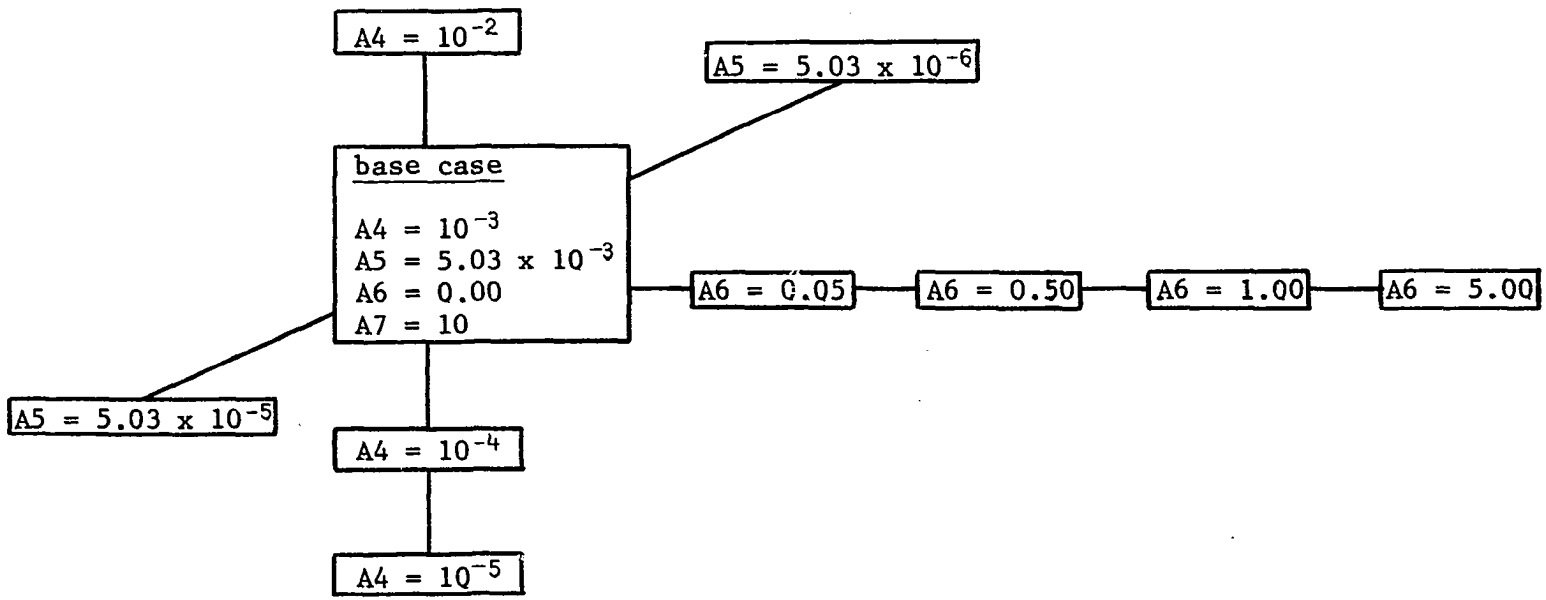

Figure 10. Values of parameters chosen for investigation of population balance model

modification is necessary to insure numerical stability in the early stages of integration. Once the first step is completed, successive integration steps are performed routinely by calling a sub-program which contains the Runge-Kutta scheme. In addition to the number density functions, the dimensionless cumulative particle concentration, P, and the dimensionless cumulative active chain concentration, R, are calculated using a simple trapezoidal rule technique. Results are printed out as called for by a counting index.

The integration is carried out until the addition to P from a single integration step contributes less than 10^{-7}% to the total value of P. At this point, the integration is terminated, the final values of P and R reported, and the system value of $\bar{n}_s$ is determined.

The program itself consumes large amounts of time in performing its assigned task. The base case, for example, required 1125 seconds to integrate to completion. Other computer runs took more or less time, depending on the values of the constants used. The integration was normally carried out over a range of about $1<\zeta<5 \times 10^4$. The volume increment used was dictated by numerical stability and was generally less than 1.0, the value being 0.10 for the base case.

There were several rules of thumb observed which might help the reader appreciate the effect the independent parameters had on the computer time required. Decreasing A4 by an order of magnitude necessitated that the integration be carried out about half an order of magnitude further along the ζ axis. Increasing A7 by an order of magnitude usually required the integration step size to be decreased by a

factor of ten. Changing the values of A5 and A6 did not appreciably affect the calculations, however increasing the value of A6 substantially would be reflected in slower operation of the program due to the extra terms which would then be included in the integration scheme.

Aside from these problems, no major difficulties were encountered in performing the following calculations. The major obstacle to obtaining more detailed solutions to the population balance equations was the enormous computation time (i.e. computer funds) required.

A4 as a Parameter

For the purpose of demonstrating the utility of the model the first six equations, generated by letting n take on the values from n = 0 to n = 5, were integrated simultaneously. It was discovered early in the work that the results were somewhat sensitive to truncation of the infinite set of equations. To minimize these effects, eleven equations were in fact integrated, while only the first six were utilized in the resulting calculations. All results presented hereafter were obtained in this manner.

Figure 11 shows the resulting particle size distributions when the calculations were performed on a dimensionless volume basis. The effect of varying values of A4 is shown in the plot, where A4 has been used as a parameter. Remember from the definition of A4 that it is proportional to the ratio of the initiator concentration to the emulsifier concentration in the feed stream, among other things.

It appears from Figure 11 that reducing A4 by factors of ten yields

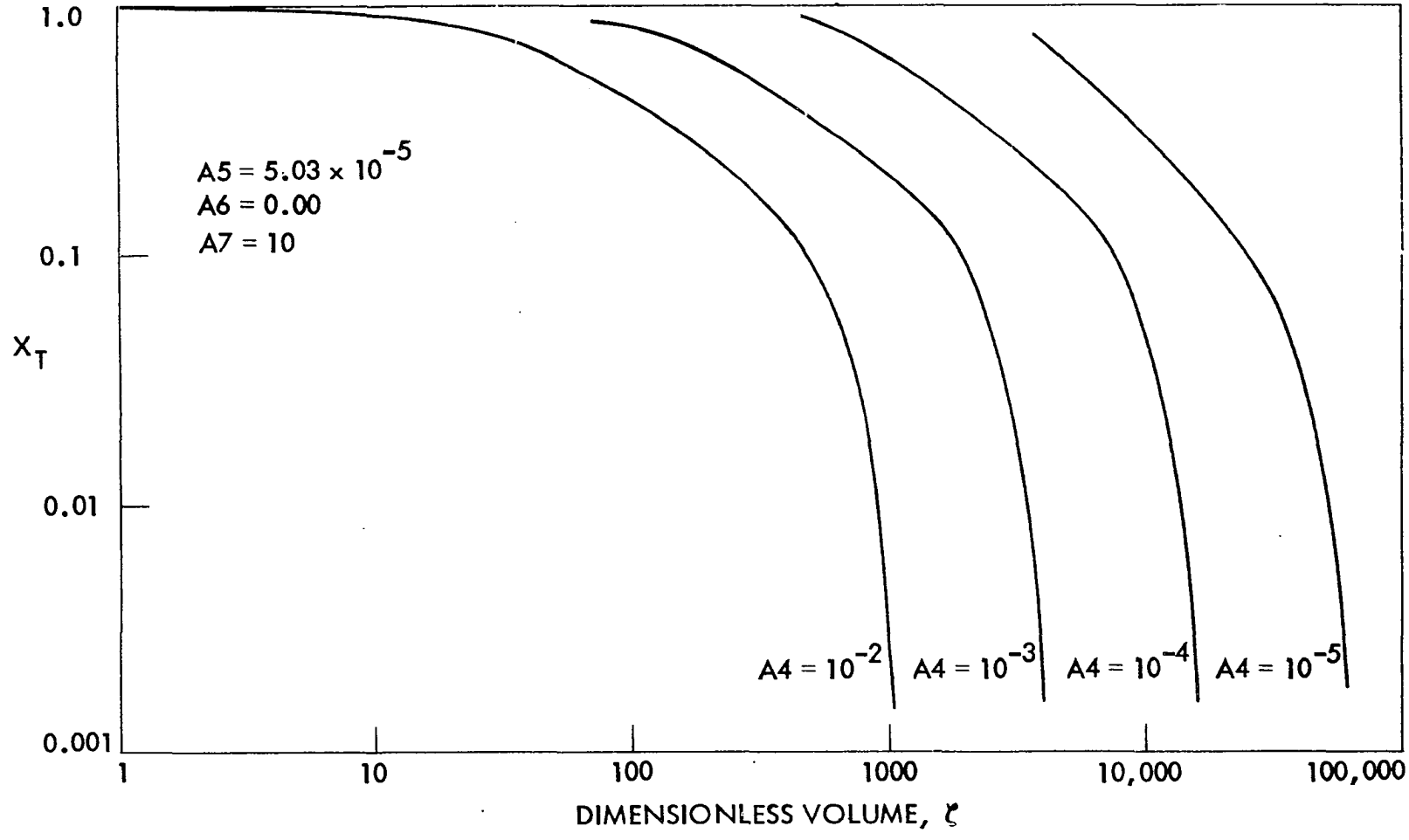

Figure 11. Volumetric particle size distributions in continuous emulsion polymerizer, demonstrating effect of parameter A4

successively greater numbers of substantially larger polymer particles. These results seem to contradict the results shown in Figure 2. The apparent discrepancy in these two figures is resolved by noting several factors.

First, and most important, the value of A7 (proportional to k_t) was purposely chosen low in order to demonstrate the effects of the slow termination rate in particles discussed by Gardon (10), in addition to minimizing computation time required of the computer. Low values of k_t allow more active polymer chains to coexist in the polymer particles before they are terminated, leading to larger particles than had the value of A7 been higher.

Secondly, as A4 decreases, the system becomes more and more starved of free radicals. Free radical arrival in the particles then slows, because absorption of radicals is proportional to the free radical concentration in the water phase. On the average, then, at low A4 values there are fewer free radicals to contribute to mutual termination in the polymer particles.

The combination of these two effects gives rise to curves as in Figure 11. Larger values of A7 would significantly increase the termination rate. Extremely high values of A7 (approaching instantaneous termination) should affect the resulting particle size distribution curves in a manner more consistent with the results in Figure 2.

Figure 12 shows how the cumulative particle size distribution varies with dimensionless particle size. That is, Figure 12 depicts the area under the X_T vs. ζ curve as a function of ζ. When the curves become

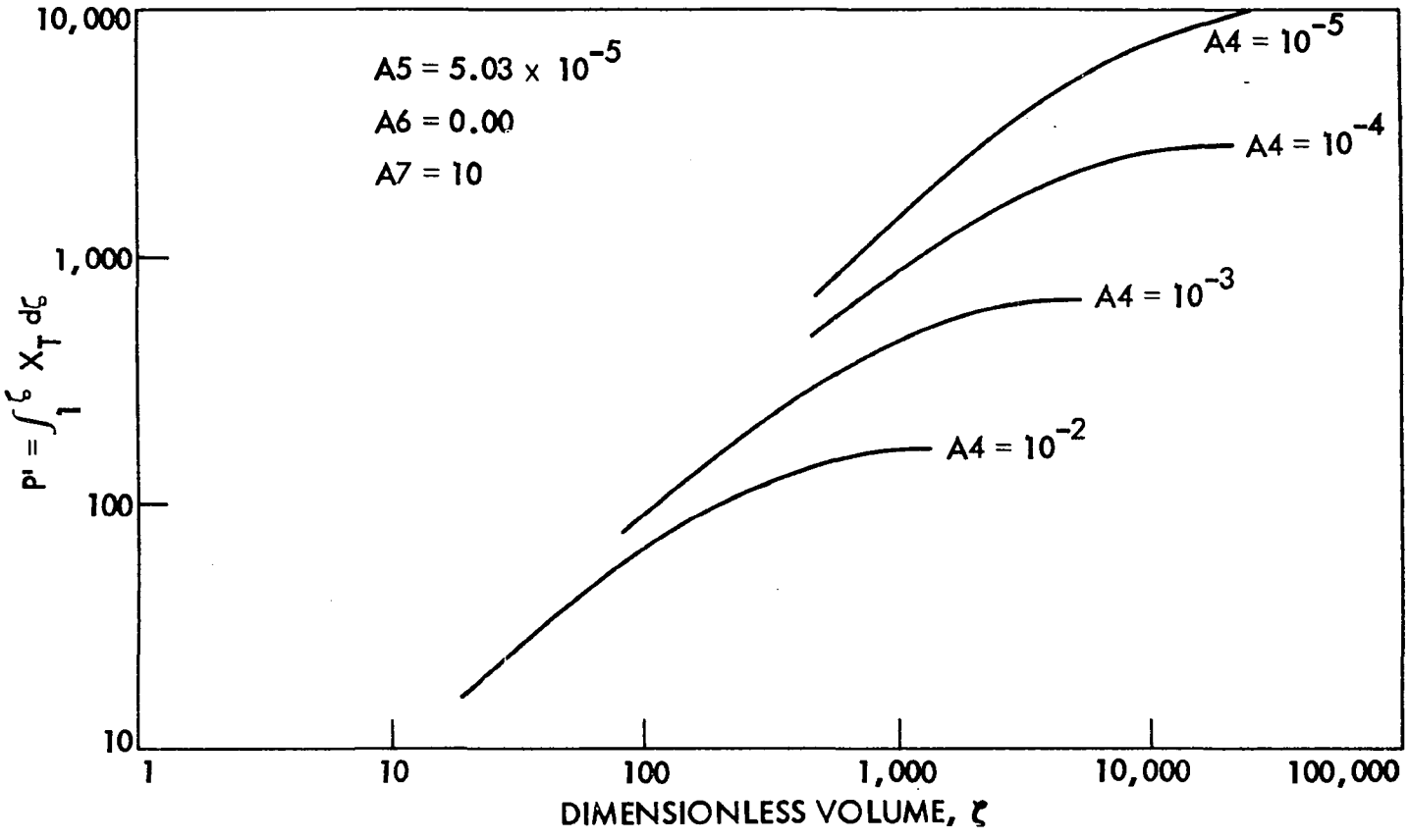

Figure 12. Cumulative dimensionless particle size distribution, showing effect of A4

horizontal lines, there are essentially no more particles being added to the total cumulative distribution. The effect of the parameter A4 is shown to be in agreement with the effect noted in Figure 11.

Figure 13 gives an indication of how the two relevant $\bar{n}$ functions vary with ζ. The size dependent value, $\bar{n}$, is shown on the upper part of the plot, while the cumulative, or "system value," $\bar{n}_s$, is shown on the lower section of the figure. The effect of A4 is demonstrated. Once again, when the curve of $\bar{n}_s$ vs. ζ becomes horizontal the integration along the particle volume axis is essentially complete.

Conceiving of A4 as being proportional to I_0, one may view $\bar{n}$ in Figure 13 in terms of a distribution of radicals between the polymer particles and the water phase. Higher values of A4 imply higher free radical generation rates. As the system becomes more flooded with radicals, Figure 13 shows that the particles become more likely to accept these radicals. (Keep in mind that the desorption mechanism is turned off, and that the rate of termination is fixed and finite valued.) Essentially, Figure 13 implies that at higher A4 values the polymer particles are forced to accept free radicals at a smaller size such that $\bar{n}$ (and $\bar{n}_s$) is higher at a given value of ζ.

Figure 14 shows the results of the system, where A4 is now the independent variable. These curves are merely a recapitulation of previous results. Plotted are the total concentration of polymer particles leaving the reactor, P, the term R, which is proportional to the overall rate of polymerization, and the system value of $\bar{n}_s$. Qualitatively, the plots of P and R vs. A4 agree with the data in Figures 9 and 10 from DeGraff's

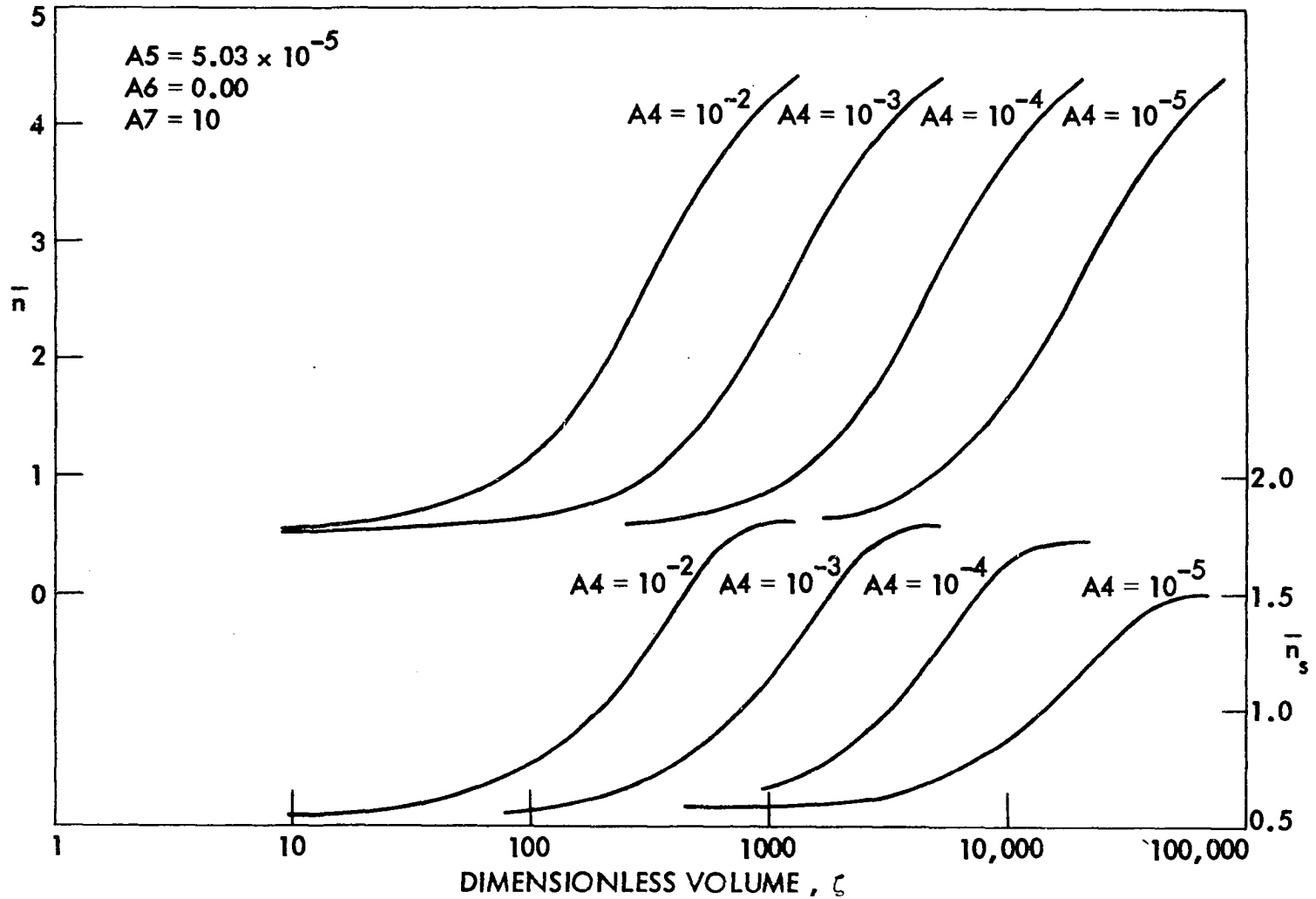

Figure 13. $\bar{n}$ and $\bar{n}_s$ as functions of particle size, illustrating the effect of A4

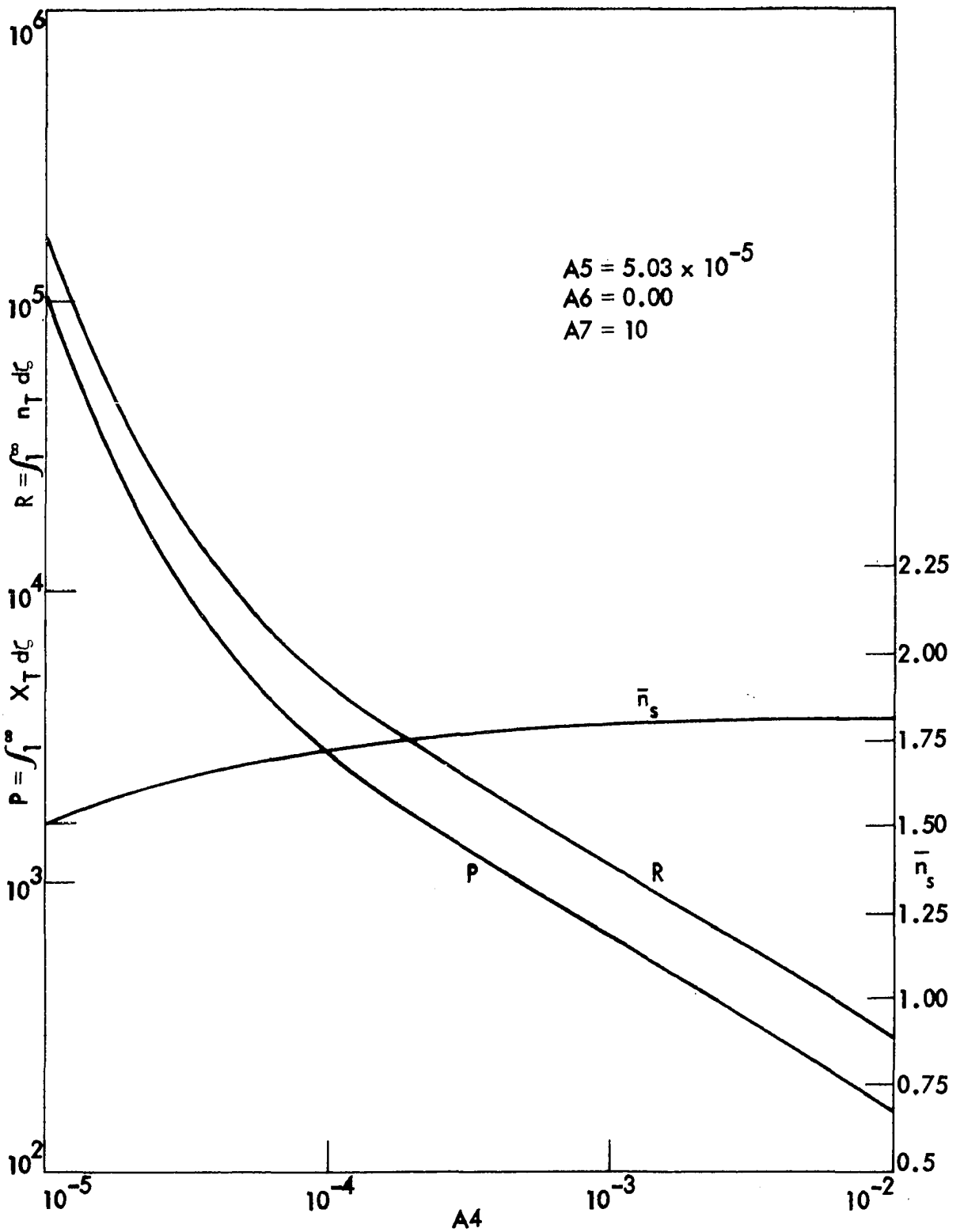

Figure 14. Overall particle concentration, active polymer chain concentration, and average number of radicals per particle as functions of A4

work (4). (See also Figure 5 of DeGraff and Poehlein (5).)

One particularly interesting feature of the present population balance model for emulsion polymerization is that when the problem has been solved, one obtains specific information of population density as a function of particle size for each particle type included in the investigation. One quickly learns which functions are important by plotting the X_n functions on the same particle size scale. Figure 15 shows these results for the base case in this study. Shown are the six X_n functions and the algebraic sum of the six, X_T, plotted on the dimensionless volume axis, ζ. It is apparent that the X_0 and X_1 functions are the only pertinent ones which need be considered until about $\zeta = 100$. At $\zeta = 1000$ the higher X_n functions begin to predominate and the contribution to X_T from X_0 and X_1 becomes increasingly less important. These results are not surprising, for one would expect larger particles to be capable of housing larger numbers of active radicals than the smaller particles. All three of the mechanisms concerning free radical activity (absorption, desorption, and termination) favor this behavior. Plots similar to those in Figure 15 give some indication of how many functions need be considered in the integration to include substantially all of the particles. Figure 15, for example, suggests that perhaps several more functions might have been included in the calculations, especially in the vicinity of $\zeta > 1000$. Figure 16 shows the results of the base case where the same eleven equations were integrated, but the first eight were used for computational purposes. For clarity, only the X_n curves for $n = 4$, 6, and 7 are shown. As expected the effect of these two added expressions is

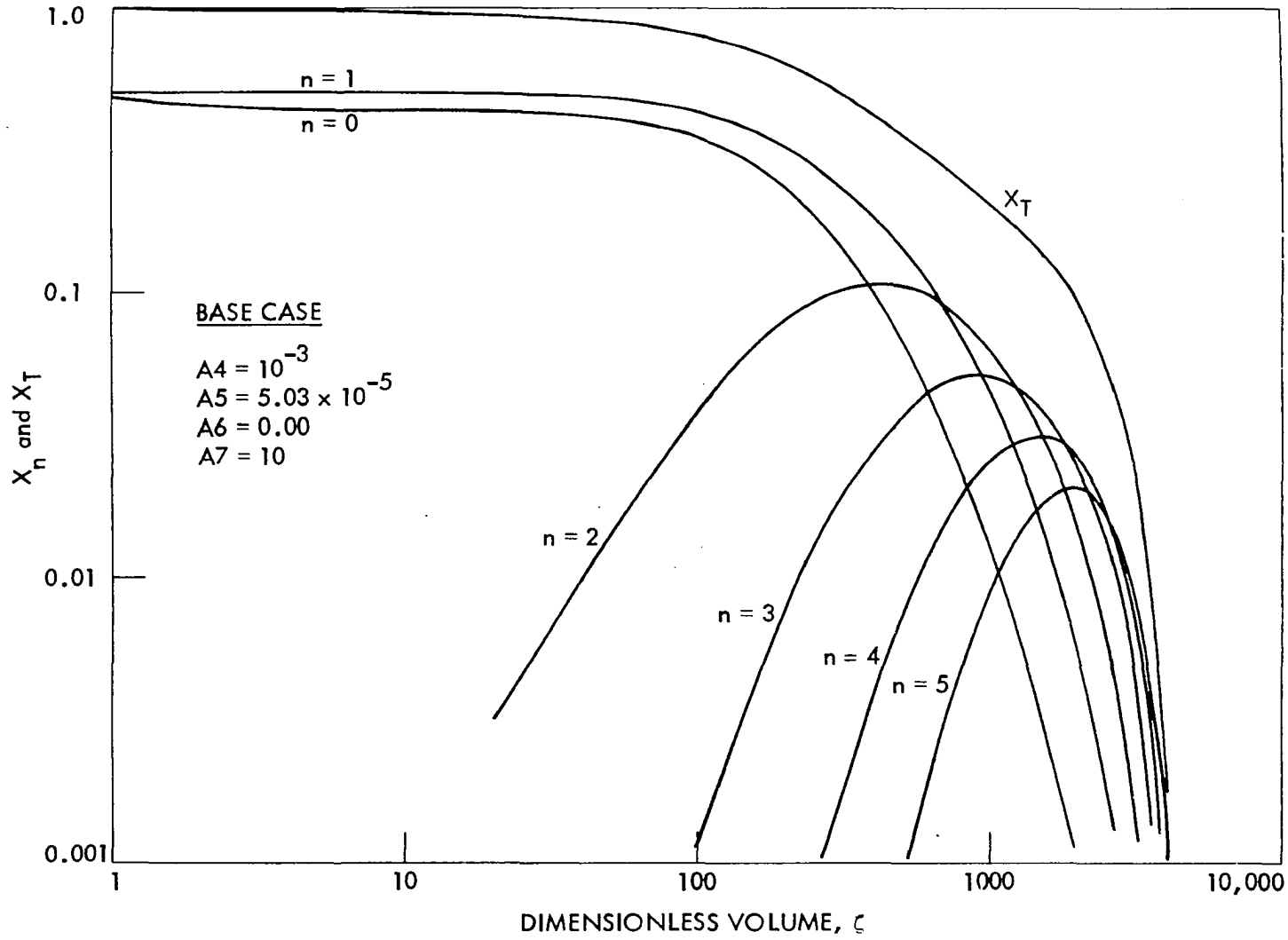

Figure 15. Particle size distribution results for X_n functions: base case

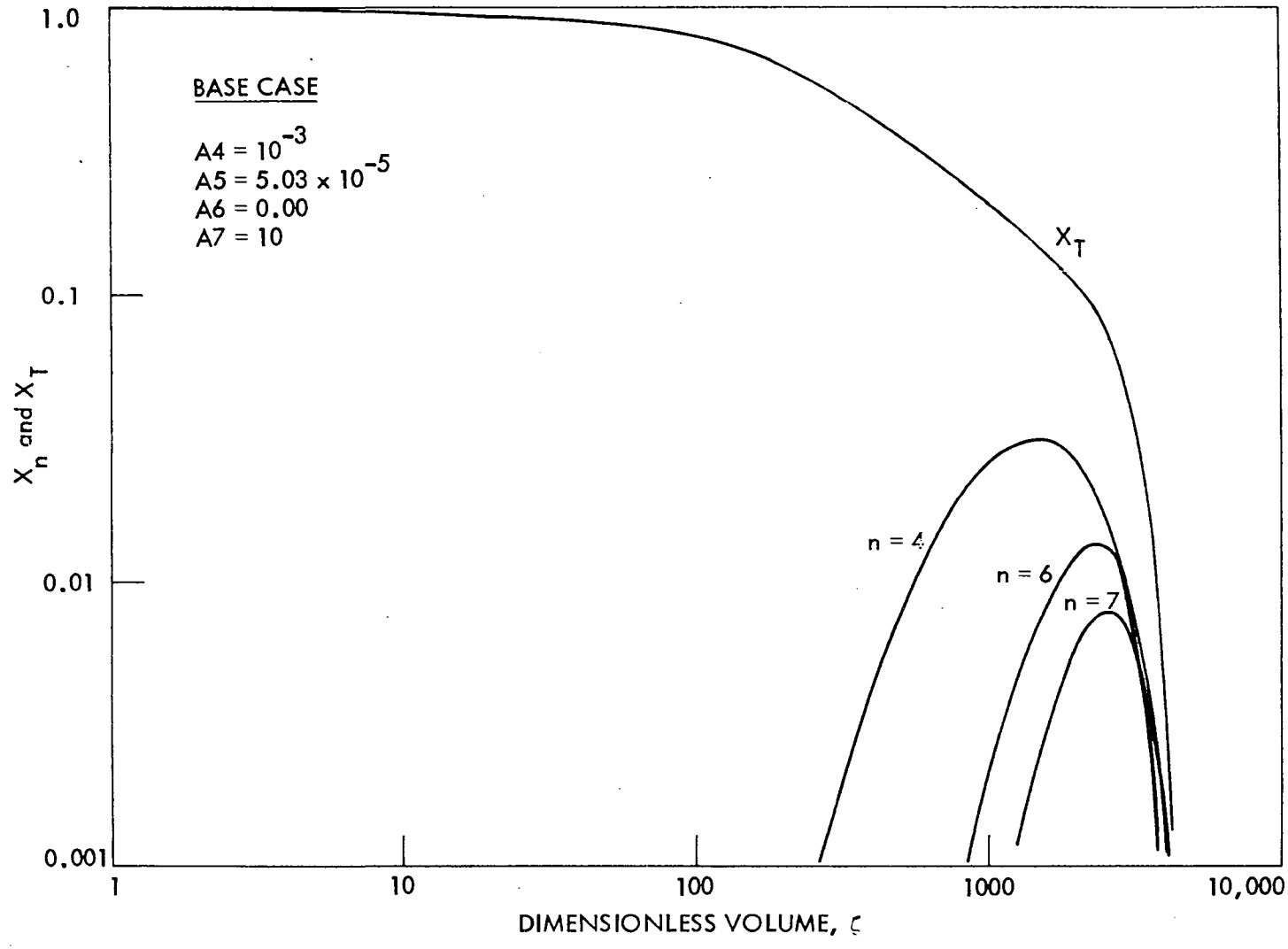

Figure 16. Effect of including X_6 and X_7 in base case particle size distribution results

negligible except at values of ζ greater than about 2000. Even above $\zeta = 2000$, the effects noted are not significant. As will be shown later, most particles formed in a typical polymerizer are well under $\zeta = 5000$ in size. (These results do not suggest that in all cases one need consider only functions up to n = 5.)

Comments on Desorption

Figure 17 shows a similar composite plot, where the desorption mechanism is now turned on by virtue of allowing A6 to take on the value of 0.05. Note first the different shape of the X_T curve. Secondly, note that the X_n curves lie much lower on the same scale than in the case where A6 = 0.00. The desorption mechanism tends to force the particles to reject free radicals such that the X_5 function does not even appear in Figure 17. Note too the different behavior in the X_0 and X_1 curves, remembering that their behavior for low values of ζ is governed by the curves shown in Figure 9. It appears that $\bar{n}$ at $\zeta = 1$ is essentially zero due to the strong effect of the desorption mechanism.

Figure 18 shows the particle size distributions for various values of the desorption parameter, A6. The other conditions are constant for each curve and are such that A6 = 0.00 represents the base case. As expected, higher magnitudes of the desorption parameter generate particles of consistently smaller size. That is, particles are allowed to grow for only short times before the radicals are forced out of the particles. Polymer particles are not allowed to house as many free radicals, on the average, when the desorption mechanism is turned on.

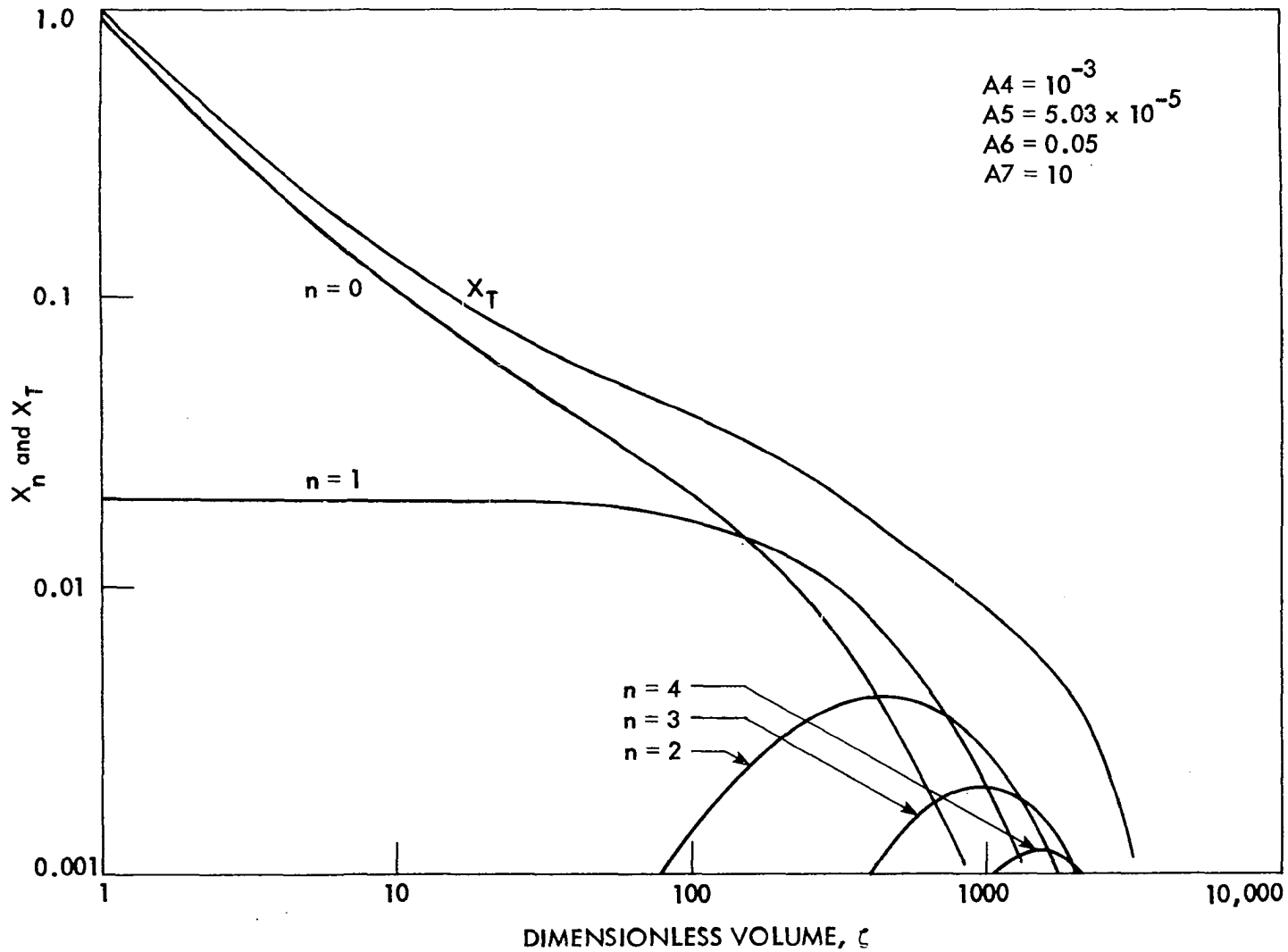

Figure 17. Particle size distribution results for X_n functions: desorption mechanism activated

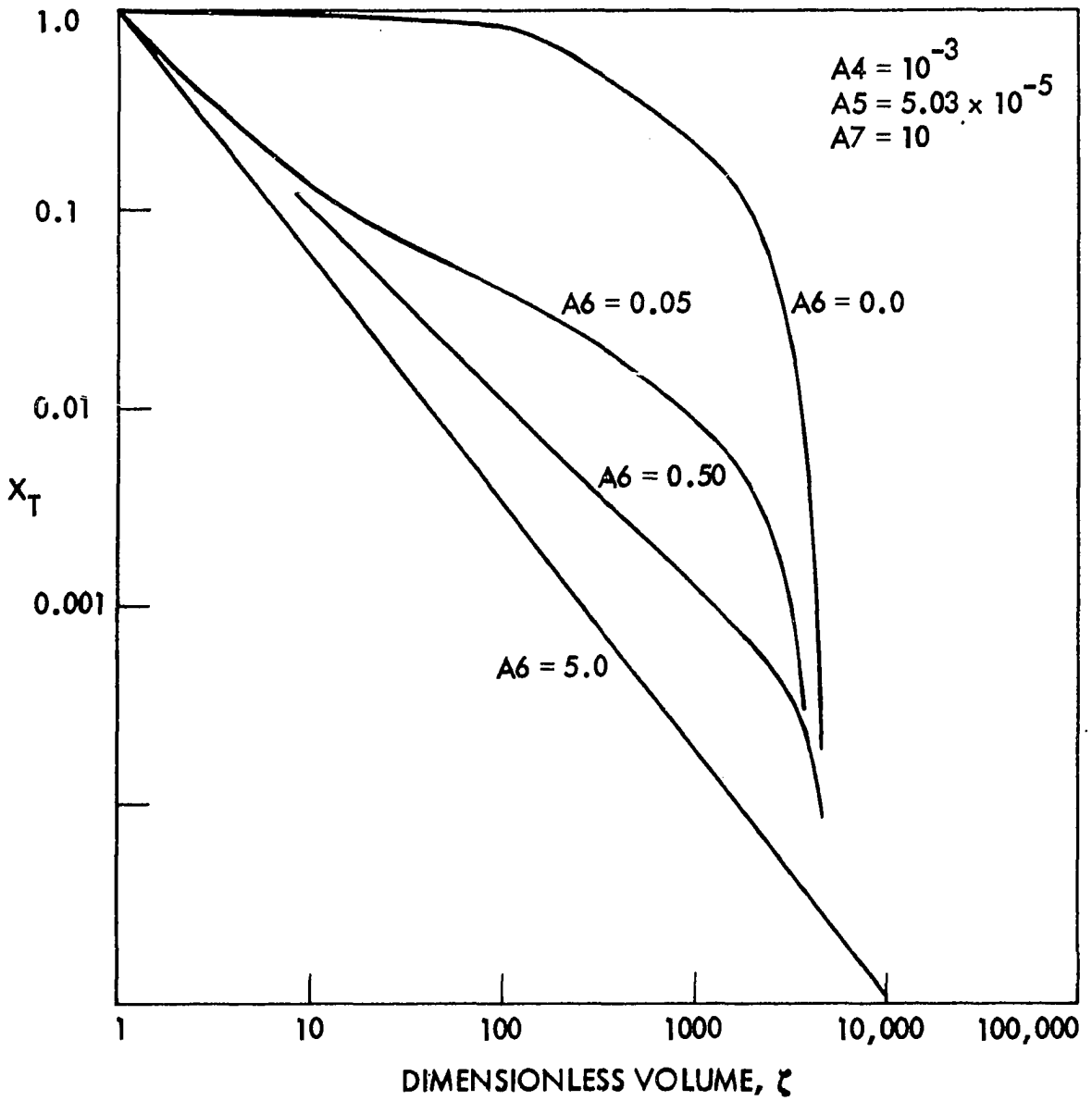

Figure 18. Particle size distributions showing the effect of the desorption mechanism

In addition, notice that it appears that the desorption mechanism leads to a product having fewer total particles as the magnitude of the mechanism increases. This result may in part be due to the use of the non-dimensionalizing variable, N_{T_0}, which may be different from one experiment to the next. However, free radicals were not assumed active once they had been desorbed. In other words, free radicals had but one chance to generate polymer in the particle. Upon termination or desorption, the activity of the free radical was finished. This part of the model is an obvious shortcoming, but it has been shown in previous work (38, 39) that to allow radicals to maintain their activity after desorption implies an iterative solution to the problem, an overwhelming task in this instance. In the present model, the rate of generation of free radicals, ρ_A, would be replaced by the free radical concentration in solution, R*, a quantity which is a function of the desorption mechanism and the particle size distribution.

Figure 19 shows plots of the size dependent average number of radicals per particle, $\bar{n}$, and the system value $\bar{n}_s$ as functions of ζ, where the desorption constant, A6, has been used as a parameter. As expected, larger values of A6 reduce the average number of radicals a particular size particle may contain. As A6 increases, radicals are forced to leave the particles at a higher rate.

The same qualitative results appear in the $\bar{n}_s$ plots. Important especially are the final values for each of the $\bar{n}_s$ curves, indicating the overall values of $\bar{n}_s$ for the system. Simply stated, the greater the magnitude of the desorption mechanism, the lower the value of $\bar{n}_s$. More

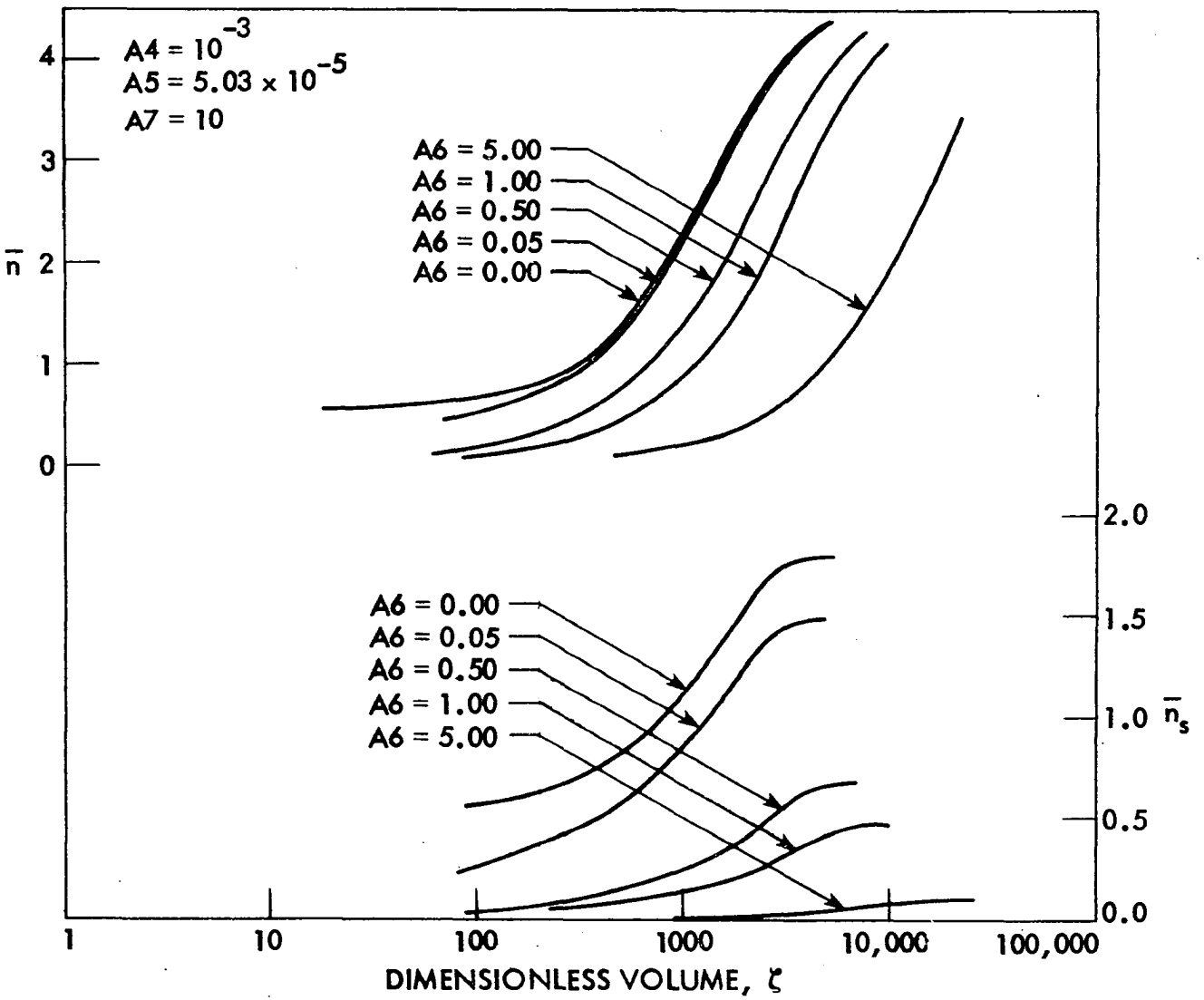

Figure 19. Effect of desorption of radicals on $\bar{n}$ and $\bar{n}_s$ from population balance model

free radicals are forced out of the polymer particles.

Effluent Levels of Initiator, Soap, and Monomer

The effluent concentrations of the other major components in the system are of interest at this point. The design of a polymerizer would not be complete without this information. These predictions become particularly important when designing several reactors in series, where additional substituents might be required in successive stages. As shown here, some of these effluent concentrations are functions of the particle size distribution. These quantities are calculable from other models and are included here for completeness.

If the initiator decomposes to give free radicals in the water phase, then the effluent concentration of initiator from the stirred tank polymerizer is given by:

$$I_1 = \frac{I_0}{1 + k_d \tau} . \tag{45}$$

At steady state, soap molecules are entering the system at a constant rate, leaving the system as soap molecules (or micelles), and leaving on the surface of polymer particles. Expressed mathematically, this conservation relation becomes:

$$S_0 - S_1 - S_c = 0. \tag{46}$$

Note that it has been assumed that a negligible amount of soap remains adsorbed on the surfaces of the monomer droplets. This assumption is probably valid at higher conversion levels. The polymer soap covering term, S_c, may be determined by assuming the polymer particles are

completely covered by a monolayer of soap molecules:

$$S_c = A_T/a_s . \tag{47}$$

But, the total polymer surface area, A_T, is given by:

$$A_T = (4\pi)^{1/3}(3)^{2/3}\int_{v_0}^{\infty} v^{2/3}N_T dv = (4\pi)^{1/3}(3)^{2/3}v_0^{5/3}N_{T_0}\int_1^{\infty}\zeta^{2/3}X_T d\zeta . \tag{48}$$

Finally, then, the effluent soap concentration is given by:

$$S_1 = S_0 - \frac{(4\pi)^{1/3}(3)^{2/3}v_0^{5/3}N_{T_0}}{a_s}\int_1^{\infty}\zeta^{2/3}X_T d\zeta . \tag{49}$$

In addition, the micelle concentration leaving the reactor may be found directly from the soap concentration to be:

$$m_1 = m_0 - \frac{(4\pi)^{1/3}(3)^{2/3}v_0^{5/3}N_{T_0}}{a_s S_9}\int_1^{\infty}\zeta^{2/3}X_T d\zeta . \tag{50}$$

The effluent micelle concentration predicted is the same whether or not the critical micelle concentration is considered.

Lastly, it is desired to predict the effluent monomer concentration. Instead, it becomes easier to examine the conversion level of monomer, Ψ, defined by:

$$\Psi \equiv 1 - M_1/M_0 . \tag{51}$$

Monomer conversion depends on the rate of polymerization in the particles. Summing over all growing particle types yields:

$$\Psi = \frac{k_p M_m \tau}{M_0 N_A} \int_{V_0}^{\infty} \left(\sum_{n=0}^{\infty} n N_n \right) dv. \tag{52}$$

According to Gardon (8) the monomer level in the polymer particles is related to the volume fraction of monomer in the particles, ϕ_M, by:

$$M_m = \frac{\rho_m \phi_M}{M_w} . \tag{53}$$

The conversion level for monomer can then be represented as:

$$\Psi = \frac{k_p \phi_M \rho_m \tau v_0 N_{T_0}}{M_0 N_A M_w} \int_{1}^{\infty} n_T d\zeta . \tag{54}$$

It has been assumed in arriving at Equation 54 that the monomer level in the particles, M_m, is the same for all particles and is invariant in time and space.

Calculation of $\bar{n}$ from Data

The experimentalist has at his disposal a quick and easy tool for analyzing his particle size distribution data. Consider the steady state population balance equation, written as:

$$\frac{d(nX_n)}{d\zeta} = - A5X_n + r_{X_n}, \tag{55}$$

where the Smith-Ewart rate is written as r_{X_n}. Summation over n, as n goes from zero to infinity, yields:

$$\frac{dn_T}{d\zeta} = - A5X_T, \tag{56}$$

where: $n_T = \sum nX_n$, $X_T = \sum X_n$, and $\sum r_{X_n} = 0$. Note that Equation 56 is identical to the starting place for Funderburk's work. Equation 56 shows immediately that n_T should be a monotonically decreasing function of ζ. Remembering that:

$$\bar{n} = \frac{nX_n}{X_n} = n_T/X_T \tag{57}$$

one may write Equation 56 as:

$$\frac{-dX_T}{\bar{n}d\zeta} + X_T\frac{dn}{d\zeta} = -A5X_T, \tag{58}$$

or:

$$\frac{d(\ln X_T)}{d\zeta} = -\left\{\frac{A5}{\bar{n}} + \frac{d(\ln \bar{n})}{d\zeta}\right\}. \tag{59}$$

Equation 59 shows that $\ln X_T$ should also be a monotonically decreasing function of ζ.

If one were to prefer working in dimensionless radial coordinates (defined as $\lambda^3 = \zeta$), an equation similar to Equation 59 might be derived as shown in the next section. Dimensionless volume coordinates were chosen to illustrate the technique.

Because of the nature of Equation 59 it is feasible to suggest that one might be able to represent particle size distribution data from a polymerizer in some functional form, as:

$$g(\zeta) \equiv \frac{d(\ln X_T)}{d\zeta}. \tag{60}$$

The function $g(\zeta)$ might be simple or complicated depending on the nature of the data. In lieu of choosing a single function, $g(\zeta)$, it might be necessary to use different functions for various intervals of the data. Irrespective of the choice of $g(\zeta)$, the technique is here presented.

Inherent in $g(\zeta)$, but not expressable directly, will be the system parameters. That is, $g(\zeta)$ will be different for sets of data where the system parameters have been varied. Nonetheless, given some particle size data it should be possible to fit these data to some simple functional form.

Introducing the definition of $g(\zeta)$ into Equation 59, one arrives at:

$$\frac{d\bar{n}}{d\zeta} + g\bar{n} = - A5, \tag{61}$$

which can be made exact by using the integrating factor, $e^{\int g d\zeta}$. Upon using this integrating factor, the solution to Equation 61 is:

$$\bar{n} = e^{-\int g d\zeta} \left\{ C - A5 \int_1^{\zeta} e^{\int g d\zeta} d\zeta \right\}, \tag{62}$$

where the constant of integration, C, is the quantity $(\bar{n}e^{\int g d\zeta})$ evaluated at $\zeta = 1.0$, and is found as discussed before. Given a functional form for $g(\zeta)$, $\bar{n} = \bar{n}(\zeta)$ may be evaluated.

Table 5 shows the results of several choices for $g(\zeta)$. Figure 20, then illustrates the effect of some of these choices on the size dependent value of $\bar{n}$.

Having once defined a useable $g(\zeta)$ and determined $\bar{n} = \bar{n}(\zeta)$, several other quantities become immediately available to the experimentalist. By

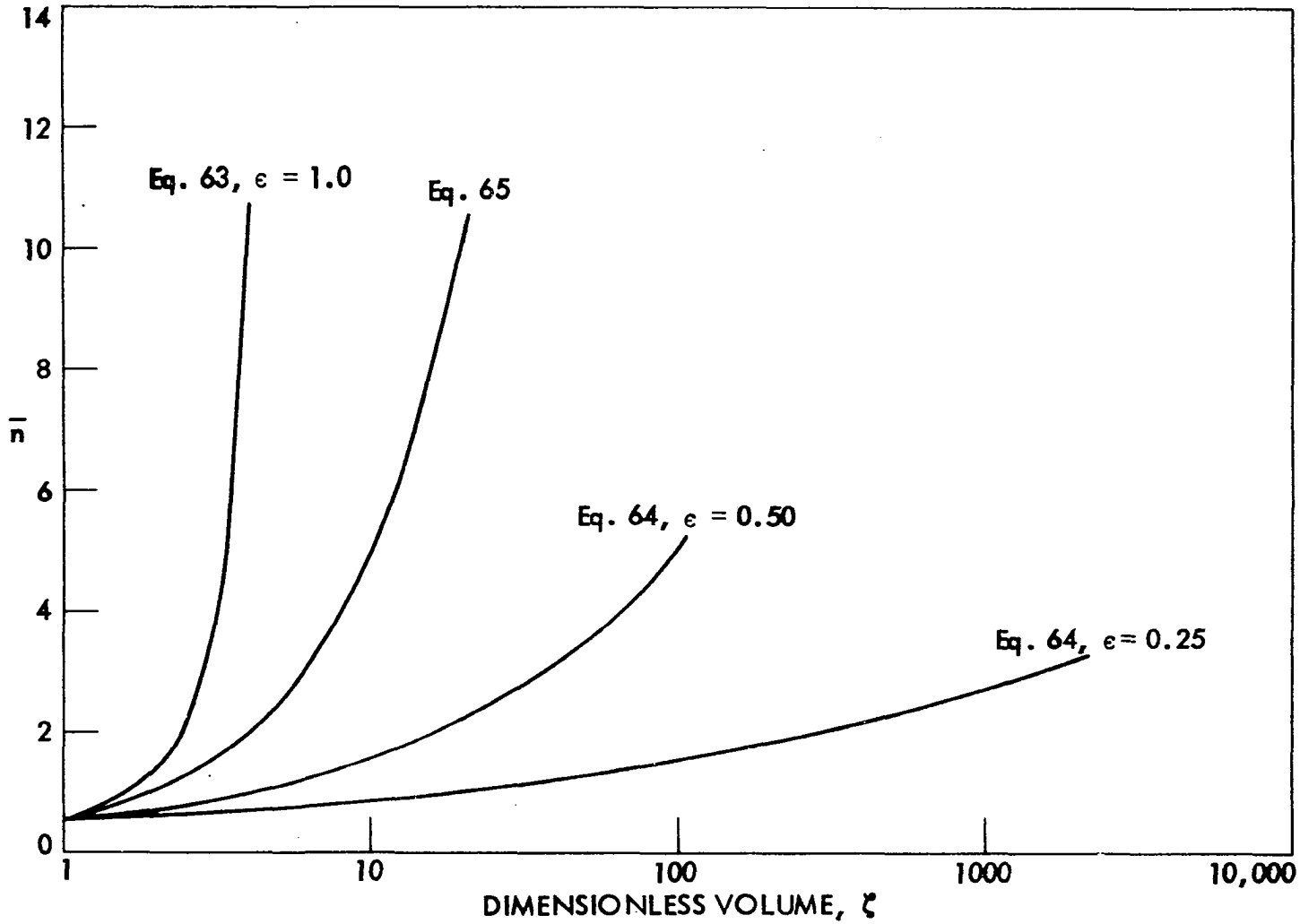

Figure 20. Illustration of "analytical estimate" technique to find $\bar{n} = \bar{n}(\zeta)$ from particle size distribution data

Table 5. Examples of the "analytical estimate" technique

$g(\zeta)$		$n = n(\zeta)$	
$-\varepsilon$	$(\varepsilon>0)$	$e^{\varepsilon\zeta}\left\{\bar{n}_1 e^{-\varepsilon} - \frac{A5}{\varepsilon}(e^{-\varepsilon} - e^{-\varepsilon\zeta})\right\}$	(63)
$-\varepsilon/\zeta$	$(\varepsilon>0, \varepsilon\neq 1)$	$\zeta^{\varepsilon}\left\{\bar{n}_1 - \frac{A5}{1-\varepsilon}(\zeta^{1-\varepsilon} - 1)\right\}$	(64)
$-1/\zeta$		$\zeta\left\{\bar{n}_1 - A5\cdot\ln\zeta\right\}$	(65)

ε - dimensionless constant

$\bar{n}_1$ - $\bar{n}$ evaluated at $\zeta = 1$, constant

analyzing one's data in the following way, the process of emulsion polymerization may be further investigated, for aside from defining $g(\zeta)$, the choice of $\bar{n}$ at $\zeta = 1$ is a parameter to be determined from a plot similar to the one in Figure 9. One could hopefully learn about the magnitude of the desorption mechanism from such endeavors.

The total dimensionless concentration of polymer particles leaving the polymerizer may be found from:

$$P = \int_1^{\infty} X_T d\zeta \tag{66}$$

The overall dimensionless concentration of active polymer chains leaving the reactor is given by:

$$R = \int_1^{\infty} n_T d\zeta = \int_1^{\infty} \bar{n} X_T d\zeta. \tag{67}$$

The overall "system value" of $\bar{n}_s$ may be found from:

$$\bar{n}_s = R/P. \tag{68}$$

Lastly, the effluent compositions of the other active components may be found by the method previously described.

This technique provides an "analytical estimate" of the emulsion polymerization process.

Conversion from Volumetric to Diametric Form

In some particular applications of the data one might wish to convert particle size data from a volumetric basis to a diametric basis, or vice versa. This manipulation of data is quite easily done as shown in the paragraphs below.

By definition of the dimensionless coordinates:

$$\zeta = v/v_0 \quad \text{and} \quad \lambda = d/d_0, \tag{69}$$

one immediately observes the following relation based on spherical particles:

$$\lambda^3 = \zeta. \tag{70}$$

Because of the units inherent in the number density function, N_T, one must make appropriate changes therein as well. Upon converting from volume to diameter coordinates, one finds that:

$$N_T(v) = \frac{6}{\pi d^2} N_T(d) \quad \text{and} \quad N_{T_0}(v) = \frac{6}{\pi d^2} N_{T_0}(d). \tag{71}$$

The ratio of these two expressions yields the dimensionless population density function relationship of:

$$X_T(\lambda) = \lambda^2 X_T(\zeta), \tag{72}$$

or:

$$X_T(\lambda) = \zeta^{2\beta} X_T(\zeta). \tag{73}$$

Lastly, one might wish to anticipate the location of relative maxima or minima in the plot of $X_T(\lambda)$ vs. λ. To seek this information, one merely sets the derivative of $X_T(\lambda)$ with respect to λ (or ζ) equal to zero, which yields:

$$\frac{d(\ln X_T(\zeta))}{d(\ln \zeta)} = -2/3 \tag{74}$$

Where the plot of $\ln X_T(\zeta)$ vs. $\ln\zeta$ has a slope of -2/3, there will the plot of $X_T(\lambda)$ vs. λ be either a relative maximum or minimum. Figure 21 shows two such plots for two values of A6, found by making the appropriate transformations from two curves found in Figure 18.

Effect of Residence Time Variations

Several computer runs were made to investigate the effect of the average residence time in the polymerizer, τ. These results are shown in Figure 22, where the overall particle size distributions are plotted. The residence time variation was manifested in changes in the parameter A5. Note that A5 is inversely proportional to τ, and it is the only independent parameter which is related to τ (see Appendix B).

The base case was used as the standard curve for comparison, i.e. when A5 = 5.03×10^{-5}. Two other values for A5 were chosen, one higher by a factor of ten and one lower by a factor of ten than the base case value of

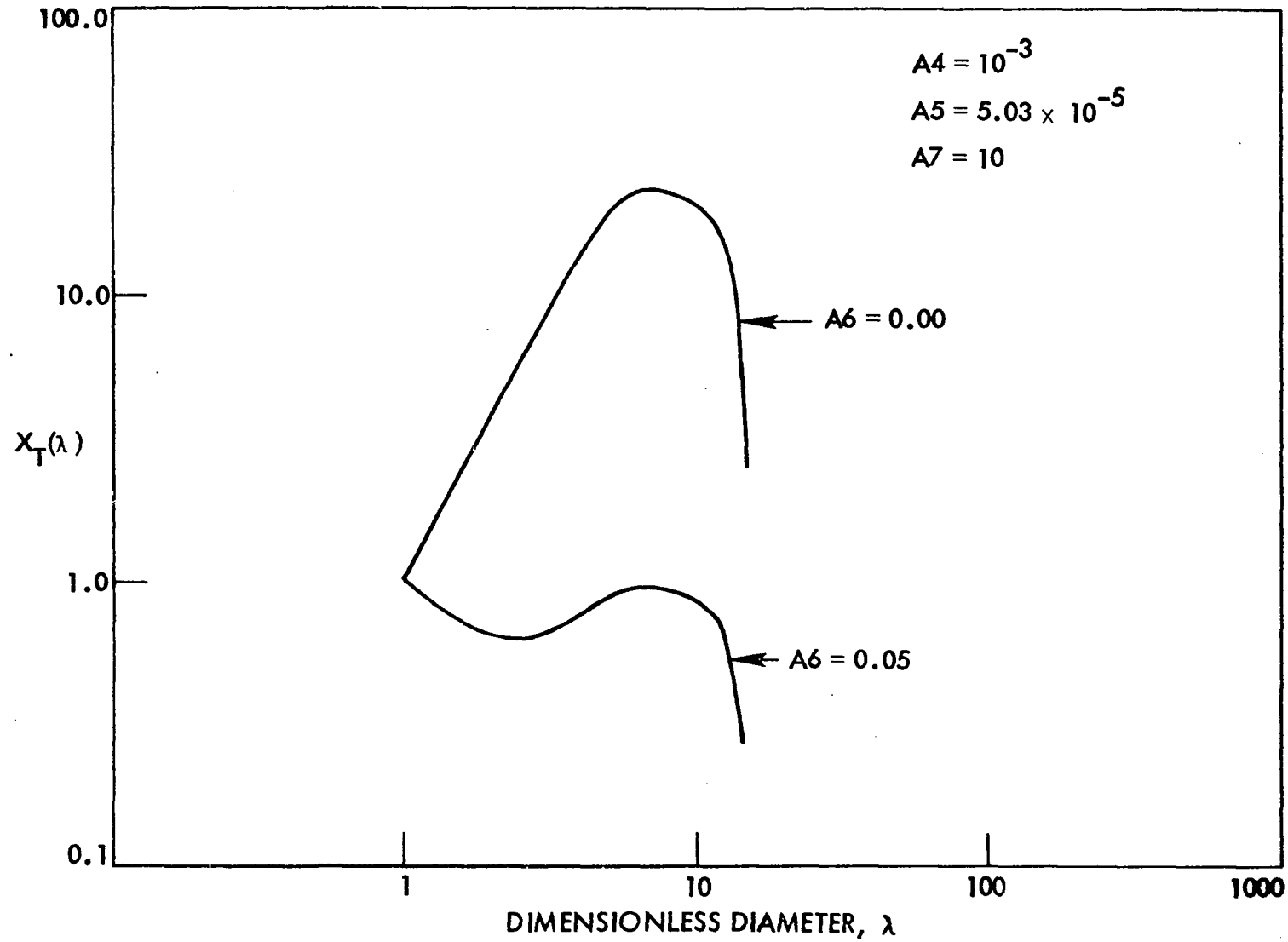

Figure 21. Particle size distributions plotted on a dimensionless diameter basis

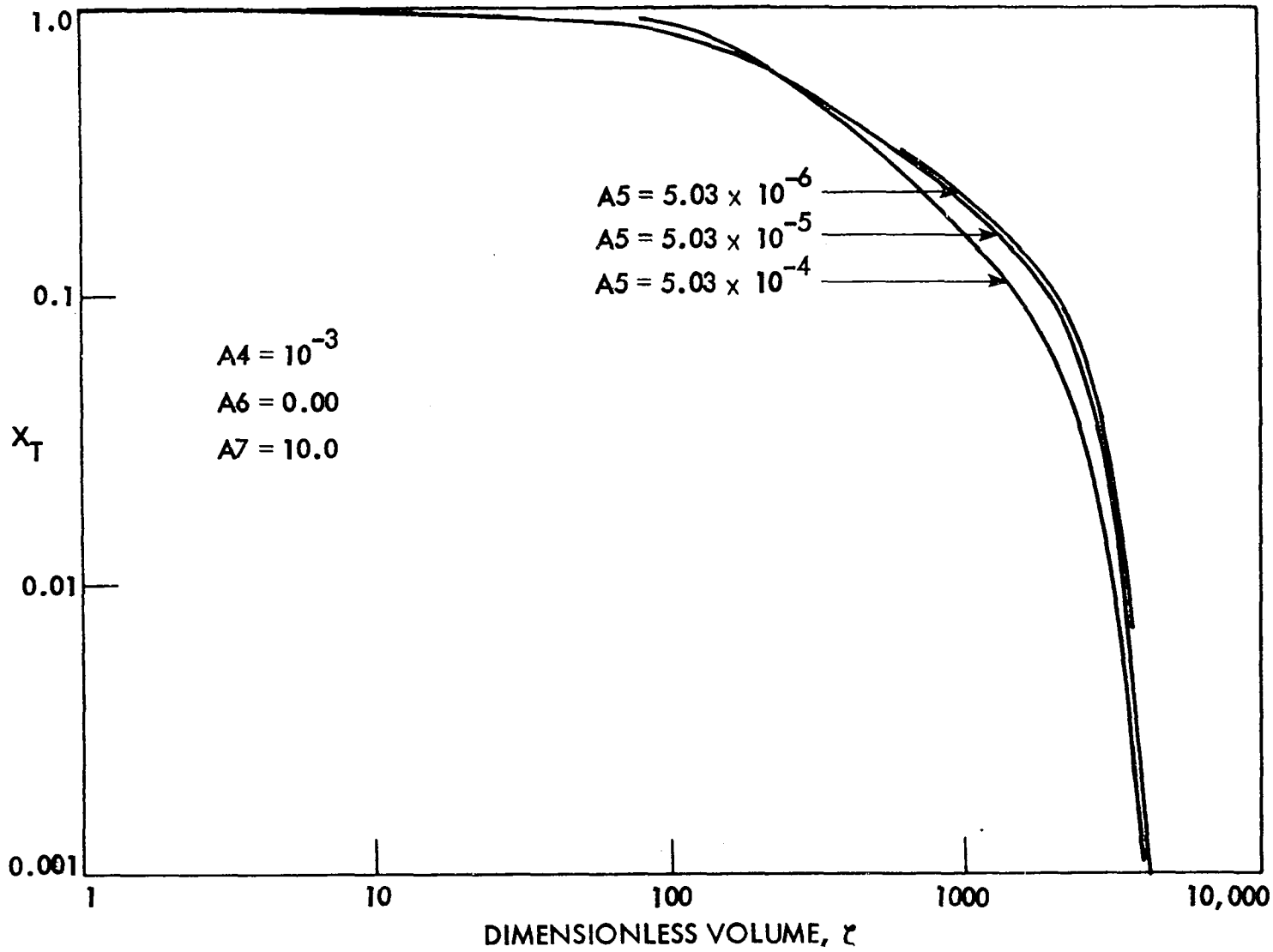

Figure 22. Effect of residence time variations on the overall particle size distribution

A5. All other independent parameters were held constant at their base case values.

There are essentially three features worth noting in Figure 22. First, the parameter A5 has more effect on the nature of the curves as it increases above the base case value. Even a value of A5 a factor of ten smaller than the base case value of A5 has little effect on the nature of the curves. Larger values of A5 would be expected to show increasingly more effect. This result implies, mathematically, that the bulk flow term in the population balance equations is becoming more important as A5 increases above the base case value of 5.03×10^{-5}. Much below this value the effect of variations in A5 appears to be negligible.

The second effect shown in Figure 22 is the way in which changes in A5 affect the shape of the curves, i.e. the nature of the particle size distribution. It appears that the higher values of A5 (lower values of τ) shift the curve up at low ζ values, while making the curve steeper at high ζ values. In other words, shorter residence times will yield latex products of a narrower size distribution having fewer larger particles, while longer residence times will produce a broader particle size distribution having more larger particles. Longer residence times will give rise to higher concentrations of larger particles at the expense of the narrow distribution produced at shorter residence times.

Thirdly, Figure 22 shows that the effect of changing τ by as much as two orders of magnitude is really not appreciable. Although the trends noted are as expected qualitatively, the particle size distribution curves exhibit a lack of sensitivity to variations in τ. Whereas two

orders of magnitude cover about the whole useful range of that variable, one might expect negligible effects in variations in τ. These statements are valid for the current choice of values of the other independent parameters. It is certainly conceivable that different values for the other parameters might make the results more sensitive to variations in A5.

Analysis of Funderburk's Run #4

One set of data was extracted from the work by Stevens and Funderburk (35). Their data from run #4 (Figure 10 in their work) was converted to a form amenable to analysis by the present model. Shown in Figure 23 are their data, as well as the predictions of the current work. Values of the constants used, as well as the calculated parameters, are shown in Appendix C.

Note that the data fall qualitatively in the same range of ζ as the theoretical curves presented in Figure 11. The extremely small value of A4 would lead one to expect the data to lie in a much larger particle size range. The larger value of A7, however, is sufficient to offset this expected effect.

Figure 23 shows that while the shape of the predicted curve conforms reasonably well with the data, actual numerical agreement is not as good as one would like. While Stevens and Funderburk manipulated two adjustable parameters to achieve an excellent fit to their data, the present model predictions were carried out using their values unaltered. There were no curve-fitting attempts.

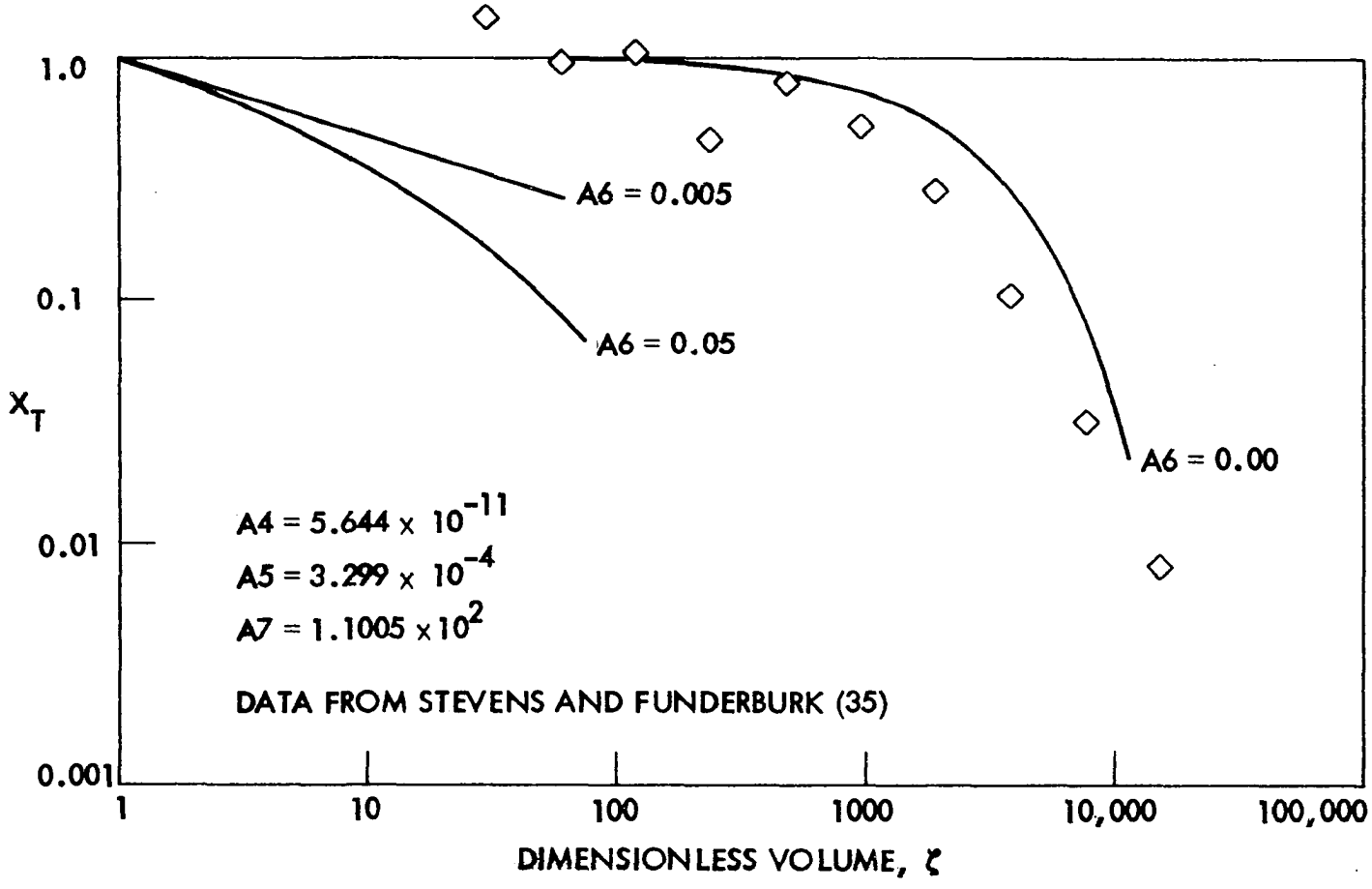

Figure 23. Population balance model predictions of data from Funderburk's run #4.

Perhaps the most questionable parameter fit done by Stevens and Funderburk was an attempt to mathematically back out the effect of an inhibitor in the system which was not physically removed before performing the experiments. The approach used was to introduce an induction time into their model which reduced the effective residence time in the polymerizer substantially. They assumed the polymer grew not at all during this induction time. The current model predictions employed their calculated effective residence time for lack of any better meaningful time. It is not at all clear that their technique is reliable or even justified. Future experiments aimed at discerning the kinetics of emulsion polymerization should certainly be done in the absence of inhibitor.

It seems logical to suggest, based on the results of Figure 22, that using a larger residence time in the predictions of these data would more adequately represent the data. A larger residence time should produce a wider distribution of particle sizes and yield more larger particles. These data seem to imply that particles may have grown in the reactor somewhat longer than the effective residence time determined by Stevens and Funderburk.

These data may also suggest that the mechanism of free radical desorption was slightly activated during the experiment. The effect of desorption, observed in Figure 18, would tend to bring the predicted curve closer to the data reported. Figure 23 shows the results of variations in model predictions when the parameter A6 was allowed to take on two non-zero values. While the effect was slightly overestimated, it is quite reasonable to postulate that free radicals were indeed desorbing from the

growing polymer particles to some slight degree. More numerical work would hopefully bear out this point and firmly establish an accurate value of A6 which would describe these data. It was not deemed fruitful to pursue this point at this time due to the uncertainty in the value of τ and the high cost of the computer simulation.

CONCLUSIONS

Two models describing emulsion polymerization processes were presented herein. The "macroscopic" model, quite simple to use, predicts overall quantities: particle concentrations, rate of polymerization, $\bar{n}_s$, etc. The population balance model requires more effort on the part of the computer, but generates individual particle-type size distribution information, from which other relevant quantities may be determined. The conclusions drawn from this study follow.

1. The mechanism of free radical desorption from polymer particles may be included quite easily in both models discussed. Whereas previous workers (4, 7) were unable to include this effect, due to inherently complicated mathematics, it is shown to add no complexity when included in either model.
2. While other workers (4, 7) were required to postulate a value for $\bar{n}$ (or $\bar{n}_s$) for their mathematical models to function, both models discussed herein find $\bar{n}$ (and/or $\bar{n}_s$) as a consequence of solutions of the model equations. Solutions of these new model equations are mathematically simpler than those of previous workers (4, 7).
3. Models presented by previous authors (4, 7) allowed them to calculate overall polymer particle results. The new population balance model predicts particle size distributions for each particle type, characterized by containing n growing polymer chains. The complexity of the model to be solved (i.e. maximum n) is dictated by the values of the independent parameters involved and is directly controlled by the individual performing the analysis.

4. The effluent compositions of the active species involved may be calculated from both models presented.
5. A technique for obtaining an "analytical estimate" of an emulsion polymerization process using particle size data was illustrated using the population balance model.
6. It was shown that the new population balance model equations may be applied to other reactor systems.
7. The parametric study done using the population balance model showed that A5 (inversely proportional to the residence time) has relatively little effect on the particle size distribution results. Variations in the values of A4 (proportional to the ratio I_0/S_0) and A6 (related to the desorption mechanism) appear to change the nature of the predicted results substantially. Cost factors limited the furtherance of the parametric study.

RECOMMENDATIONS FOR FUTURE WORK

As with many research projects the efforts to date have left unanswered questions. The results of investigations thus far reveal that there remains much work to do. What follows is a list of further activities conceived at this writing:

1. Although by numerical integration one can visualize which functions are important in the population balance model, this method only yields information after the fact. A significant contribution would be to establish some means of determining á priori how many functions need be included in the integration scheme to yield accurate and meaningful results.
2. No work has yet been performed on the equations governing the batch reactor. Certainly these population balance equations suggest that much stands to be learned about the individual particle types and the effects of the inherent mechanisms on them.

   The full transient batch reactor equation is:

$$\frac{\partial X_n}{\partial \theta} + \frac{\partial (n X_n)}{\partial \zeta} = r_{X_n}, \tag{75}$$

   where θ is a dimensionless time defined as:

$$\theta \equiv \frac{Kt}{v_0}, \tag{76}$$

where r_{X_n} is here expressed in the dimensionless form, and K has been assumed independent of particle volume, ζ. Summing over all particle types gives:

$$\frac{\partial X_T}{\partial \theta} + \frac{\partial (\bar{n} X_T)}{\partial \zeta} = 0. \tag{77}$$

When all the particles are formed, X_T is independent of time, so:

$$\frac{d(\bar{n} X_T)}{d\zeta} = 0. \tag{78}$$

Equation 78 does not imply that $\bar{n}$ is invariant in time. One suspects that the free radical distribution in the particles will change with time (i.e. $X_n = X_n(t)$), so that $\bar{n}$ will change with time. As a result, to obtain information for the batch system, one must solve the component balances described by Equation 75.

3. The generating function approach introduced by Stockmayer (36) might be used to solve both the batch and continuous reactor equations developed here. By defining a generating function as:

$$f \equiv \sum_{n=0}^{\infty} N_n \eta^n \tag{79}$$

Equation 34 may be multiplied by η^n and summed on n as n goes from zero to infinity to arrive at:

$$\frac{\partial f}{\partial t} + \frac{\partial}{\partial v}(Kf') = \frac{-f}{\tau} + \frac{\alpha}{v}(1-\eta^2)f'' + \beta v^{2/3}(1-\eta)f' + \frac{\gamma}{v^{1/3}}(1-\eta)f, \tag{80}$$

where the primes denote differentiation with respect to the dummy variable, η. Once having described the function $f = f(v, t, \eta)$, recall from Stockmayer that (36):

$$\bar{n} = \frac{f'/_{\eta=1}}{f/_{\eta=1}} = \bar{n}(v, t). \tag{81}$$

The quantity $\bar{n}$ would be some indication of the nature of the

polymerization taking place in the reactor. In addition to evaluating $\bar{n}$, one might invert the summation in Equation (79) to learn something about the individual N_n functions using:

$$N_n = \frac{f^{n}(v, t, \eta)}{n!}/\eta=0, \qquad (82)$$

where the n-fold differentiation is to be carried out with respect to the variable η.

4. Now that a new model has been developed it appears timely to suggest building a polymerizer in which to conduct experiments. Careful design should allow for batch or continuous operation in the same reactor. All inhibitor should be removed from the feedstocks. Particle size distributions should be measured under different conditions. The number density of particles at "zero size" should be measured, not adjusted as a parameter. The data should be viewed in terms of both models discussed herein.
5. The effluent levels of the other components leaving the reactor should be measured experimentally and compared to predictions of the two models presented herein. The effluent concentration of free radicals is of particular importance because of the role they play in emulsion polymerization.

   In addition, it would be helpful to be able to include free radicals which have desorbed from polymer particles as active radicals which might again participate in polymerization. This inclusion would certainly make the population balance model more realistic.
6. There has been some evidence reported in the literature (2, 21) to

suggest that under certain circumstances a continuous stirred tank emulsion polymerizer cannot attain steady state operation, but must oscillate around a limit cycle. The transient forms of the models presented should be examined in this regard to determine under what conditions a limit cycle may arise, followed by experiments to verify these findings.

7. It was assumed throughout that K, the growth rate parameter, was invariant with respect to particle size. There is some speculation that some parameters making up K may be particle size dependent (13). This claim should be investigated. The population balance model is sufficiently general to review this assumption.
8. During the course of this work, it was assumed that there was no polymer in the feed stream. The models are sufficiently general to include analysis of a system which had polymer in the feed, for example several stirred tank polymerizers in series. This problem might be investigated as it has some industrial significance.

LITERATURE CITED

1. Behnken, D. W., J. Horowitz, and S. Katz. 1963. Particle Growth Processes. I&EC Fundamentals 2: 212-216.

2. Berens, A. R. 1974. Continuous Emulsion Polymerization of Vinyl Chloride. J. Appl. Poly. Sci. 18: 2379-2390.

3. Billmeyer, F. W. 1971. Textbook of Polymer Science. John Wiley & Sons, New York, 598pp.

4. DeGraff, A. W. 1970. Continuous Emulsion Polymerization of Styrene in One Stirred Tank Reactor. Ph.D. thesis. Lehigh University (Libr. Congr. Card No. Mic. 70-26,139). 184pp. University Microfilms, Ann Arbor, Michigan.

5. DeGraff, A. W. and G. W. Poehlein. 1971. Emulsion Polymerization of Styrene in a Single Continuous Stirred-Tank Reactor. J. Poly. Sci.: Part A-2, 9: 1955-1976.

6. Flory, P. J. 1953. Principles of Polymer Chemistry. Cornell University Press, Ithaca, New York. 672pp.

7. Funderburk, J. O. 1969. Polymer Particle Size Distributions in Continuous Emulsion Polymerization. Ph.D. thesis. Iowa State University, Ames, Iowa. 141pp.

8. Gardon, J. L. 1968. Emulsion Polymerization. I. Recalculation and Extension of the Smith-Ewart Theory. J. Poly. Sci.: Part A-1, 6: 623-641.

9. Gardon, J. L. 1968. Emulsion Polymerization. II. Review of Experimental Data in the Context of the Revised Smith-Ewart Theory. J. Poly. Sci.: Part A-1, 6: 643-664.

10. Gardon, J. L. 1968. Emulsion Polymerization. III. Theoretical Prediction of the Effects of Slow Termination Rate Within Latex Particles. J. Poly. Sci.: Part A-1, 6: 665-685.

11. Gardon, J. L. 1968. Emulsion Polymerization. IV. Experimental Verification of the Theory Based on Slow Termination Rate Within Latex Particles. J. Poly. Sci.: Part A-1, 6: 687-710.

12. Gardon, J. L. 1968. Emulsion Polymerization. V. Lowest Theoretical Limits of the Ratio k_t/k_p. J. Poly. Sci.: Part A-1, 6: 2853-2857.

13. Gardon, J. L. 1968. Emulsion Polymerization. VI. Concentration of Monomers in Latex Particles. J. Poly. Sci.: Part A-1, 6: 2859-2879.

14. Gerrens, H. and K. Kuchner. 1970. Continuous Emulsion Polymerization of Styrene and Methyl Acrylate. Br. Polym. J. 2: 18-24.

15. Gershberg, D. B. and J. E. Longfield. 1961. Kinetics of Continuous Emulsion Polymerization. Unpublished paper presented at the Symposium on Polymerization Kinetics and Catalyst Systems, 54th AIChE Meeting, New York. preprint No. 10.

16. Harkins, W. D. 1947. A General Theory of the Mechanism of Emulsion Polymerization. J. Amer. Chem. Soc. 69: 1428-1444.

17. Hulburt, H. M. and S. Katz. 1964. Some Problems in Particle Technology: A Statistical Mechanical Formulation. Chem. Eng. Sci. 19: 555-574.

18. Katz, S., R. Shinnar, and G. Saidel. 1969. Molecular Weight Distribution for Polymerization in a Two-Phase System. Pages 145-157 in Robert F. Gould, ed. Addition and Condensation Polymerization Processes (Advances in Chemistry Series, Vol. 91). American Chemical Society, Washington, D.C.

19. Litt, M., R. Patsiga, and V. Stannett. 1970. Emulsion Polymerization of Vinyl Acetate. II. J. Poly. Sci.: Part A-1, 8: 3607-3619.

20. Nomura, N., H. Kajima, M. Harada, W. Eguchi, and S. Nagata. 1971. Continuous Flow Operation in Emulsion Polymerization of Styrene. J. Appl. Poly. Sci. 15: 675-691.

21. Omi, Shinzo, Teiji Ueda, and Hiroshi Kubota. 1969. Continuous Operation of Emulsion Polymerization of Styrene. J. Chem. Eng. Japan, 2, 2: 193-198.

22. O'Toole, J. T. 1965. Kinetics of Emulsion Polymerization. J. Appl. Poly. Sci. 9: 1291-1297.

23. O'Toole, J. T. 1969. Stochastic Contributions to Latex Polydispersity. J. Poly. Sci.: Part C, 27: 171-182.

24. Poehlein, G. W. 1973. Advances in Emulsion Polymerization and Latex Technology. 4th Annual Short Course, Lehigh University.

25. Poehlein, G. W. and J. W. Vanderhoff. 1973. Competitive Growth of Polystyrene Latex Particles: Theory and Experiment. J. Poly. Sci.: Polymer Chemistry Edition, 11: 447-452-

26. Randolph, A. D. and M. A. Larson. 1962. Transient and Steady State Size Distributions in Continuous Mixed Suspension Crystallizers. AIChE J. 8: 639-645.

27. Randolph, A. D. and M. A. Larson. 1971. Theory of Particulate Processes. Academic Press, New York. 251pp.

28. Roe, C. P. 1968. Surface Chemistry Aspects of Emulsion Polymerization. I&EC 60, 9: 20-33.

29. Romatowski, J. amd G. V. Schultz. 1965. Emulsionspolymerisation von Styrol mit Intermittierender Radikalerzeugung. II Kinetische Untersuchungen. Die Makromol. Chem. 85: 227-248.

30. Saidel, G. M. and S. Katz. 1969. Emulsion Polymerization: A Stochastic Approach to the Polymer Size Distribution. J. Poly. Sci.: Part C, 27: 149-169.

31. Sato, T. and I. Taniyama. 1965. Kinetics of Emulsion Polymerization. Kogyo Kagaku Zasshi 68: 67-72.

32. Sato, T. and I. Taniyama. 1965. Continuous Emulsion Polymerization. Kogyo Kagaku Zasshi 68: 106-109.

33. Smith, W. V. and R. H. Ewart. 1948. Kinetics of Emulsion Polymerization. J. Chem. Phys. 16: 592-599.

34. Stevens, J. D. and J. P. Davitt. 1974. Withdrawal Behavior of Suspensions of Nearly Neutral Buoyancy. I&EC Fundamentals 13, 9: 263-267.

35. Stevens, J. D. and J. O. Funderburk. 1972. Design Models for Continuous Emulsion Polymerization and Preliminary Experimental Evaluation. I&EC Proc. Des. & Dev. 11: 360-369.

36. Stockmayer, W. H. 1957. Note on the Kinetics of Emulsion Polymerization. J. Poly. Sci. 24: 314-317.

37. Sundberg, D. C. and J. D. Eliassen. 1971. The Prediction of Size and Molecular Weight Distributions in Emulsion Polymerization. Pages 153-161 in R. M. Fitch, ed. Polymer Colloids. Plenum Press, New York, New York.

38. Thompson, R. W. and J. D. Stevens. 1975. Free Radical Desorption in Continuous Emulsion Polymerization. Chem. Eng. Sci. 30: 663-668.

39. Ugelstad, J., P. C. Mork, and J. O. Aasen. 1967. Kinetics of Emulsion Polymerization. J. Poly. Sci.: Part A-1, 5: 2281-2287.

40. Ugelstad, J., P. C. Mork, P. Dahl, and P. Rangnes. 1969. A Kinetic Investigation of the Emulsion Polymerization of Vinyl Chloride. J. Poly. Sci.: Part C, 27: 49-68.

41. Williams, D. J. 1971. Polymer Science and Engineering. Prentice Hall, Englewood Cliffs, New Jersey. 401pp.

ACKNOWLEDGEMENTS

Without help from many people and organizations, this work would likely not have gotten done by the present author. While one name appears as the author to this work, countless other individuals deserve credit.

During the course of the work, financial support has been given by the DuPont, Union Carbide, and Proctor and Gamble companies. The support by the Engineering Research Institute at Iowa State University is also appreciated.

The five members of my graduate committee were a veritable asset to the pursuit of perfection. I owe personal thanks to the following: Dr. B. C. Carlson, Dr. J. H. Espenson, Dr. R. S. Hansen, Dr. F. O. Shuck, and Dr. M. A. Larson.

Dr. John D. Stevens has been a constant supporter and stabilizing factor during these three years, serving as the director of this research. His advice, beyond merely the academic, has guaranteed continuity and sanity. Let me here express my gratitude for having had his guidance. He will simply have to adjust to having so much free time.

Lastly, my wife and daughter deserve a heart-felt thanks for enduring these years. I extend my thanks and apologies for having furthered my own career at the expense of Brenda's, and hope that in the future reimbursement may be made.

APPENDIX A. SATO-TANIYAMA DEVELOPMENT

In regards to the "macroscopic" model discussed earlier, it is desired to solve Equations (11) - (17) simultaneously. The goal of such efforts would be to predict effluent concentrations of the active species (I_1, M_1, m_1, N_1, N_1^*, R*, and N) as functions of the system parameters. Description of the technique employed follows.

For brevity the relation will be used throughout that: $K_j = k_i\tau$. That is, K_j represents the corresponding rate constant, k_j, multiplied by the average residence time in the reactor, τ.

From Equation (11) the effluent initiator concentration is found as:

$$I_1 = \frac{I_0}{1 + K_d} . \tag{A-1}$$

Equation (14) yields for the free radical concentration:

$$\bar{R}^* = \frac{K_d F I_1 + K_o N_1^*}{1.0 + K_i m_1 + K_i N_1 + K_t N_1^*} . \tag{A-2}$$

A relationship between live and dead polymer particles arises from Equation (15):

$$N_1 = \left\{ \frac{K_o + K_t R^*}{1.0 + K_i R^*} \right\} N_1^* . \tag{A-3}$$

By employing Equation (17), both live and dead particle concentrations are related to the total particle concentration:

$$N_1 = \left\{ \frac{K_t R^* + K_o}{1.0 + K_i R^* + K_t R^* + K_o} \right\} N \quad , \text{ and} \tag{A-4}$$

$$N_1^* = \left\{ \frac{1.0 + K_i R^*}{1.0 + K_i R^* + K_t R^* + K_o} \right\} N \ . \qquad \text{(A-5)}$$

Equation (12) may be easily arranged to give:

$$M_0 - M_1 = K_p M_m N_1^* \ , \qquad \text{(A-6)}$$

which is substituted directly into Equation (13) to yield:

$$m_0 - m_1 - K_i R^* m_1 - K_v (K_p M_m N_1^*)^{-1/3} N^{1/3} N_1^* = 0, \qquad \text{(A-7)}$$

which may be manipulated by using Equation (A-5) to give:

$$m_1 = \frac{m_0 - K_v \left\{ \frac{1.0 + K_i R^*}{1.0 + K_o + K_i R^* + K_t R^*} \right\} \left\{ \frac{1.0 + K_o + K_i R^* + K_t R^*}{K_p M_m (1.0 + K_i R^*)} \right\}^{1/3}}{(1.0 + K_i R^*)} \qquad \text{(A-8)}$$

Equations (17) and (A-5) may be substituted into Equation (A-6) to yield the result that:

$$N = K_i R^* m_1, \qquad \text{(A-9)}$$

which, when combined with Equation (A-8), gives:

$$N = \left\{ \frac{m_0}{1.0 + K_i R^*} \right\} \qquad \text{(A-10)}$$

$$\times \left\{ \frac{K_i R^* (1.0 + K_o + K_i R^* + K_t R^*)}{1.0 + K_o + K_i R^* + K_t R^* + K_v K_i R^* \left\{ \frac{1.0 + K_o + K_i R^* + K_t R^*}{K_p M_m (1.0 + K_i R^*)} \right\}^{1/3}} \right\}$$

and:

$$m_1 = N/K_i R^*. \qquad \text{(A-11)}$$

Equations (A-2), (A-4), (A-5), (A-10), and (A-11) each involve R*. Unfortunately, no analytical solution could be found for these equations. An iterative scheme involving these five equations was developed. The computer routine usually converged rapidly to the limiting tolerance of 0.10 percent for successive values of R*.

APPENDIX B. DEFINITION OF DIMENSIONLESS PARAMETERS

Seven dimensionless constants were used in the solution of the population balance equations. They are listed here for the convenience of the reader.

$$A4 = 2(4\pi)^{1/3}(3)^{2/3}\frac{N_A^2 k_d \rho_p v_0^{5/3}(1-\phi_M) I_0}{a_s k_p \rho_m \phi_M (1.0+K_d) S_0}$$

$$A5 = \frac{N_A v_0 \rho_p (1-\phi_M)}{k_p \tau \rho_m \phi_M}$$

$$A6 = (4\pi)^{1/3}(3)^{2/3}\frac{k_o N_A v_0 \rho_p (1-\phi_M)}{k_p \rho_m \phi_M}$$

$$A7 = \frac{k_t \rho_p (1-\phi_M)}{k_p \rho_m \phi_M}$$

$$A1 = A6/A5$$

$$A2 = A7/A5$$

$$A3 = A4/A5$$

APPENDIX C. NUMERICAL VALUES FROM FUNDERBURK'S WORK

Below are the values of the constants required to analyze run #4 from Funderburk's work (7).

a_s	3.674×10^{9}	cm^2/gm mole
I_0	1.873×10^{-6}	gm mole/cm^3
k_d	7.322×10^{-7}	1/hr
k_p	6.336×10^{8}	cm^3/gm mole hr
k_t	8.93×10^{10}	cm^3/gm mole hr
N_{T_0}	3.39×10^{12}	#/cm^6
S_0	6.153×10^{-5}	gm mole/cm^3
V	2800	cm^3
v_0	10^{-19}	cm^3
ρ_m	0.905	gm/cm^3
ρ_p	1.06	gm/cm^3
τ	0.225	hr
ϕ_M	0.60	(dimensionless)

APPENDIX D. POPULATION BALANCE PROGRAM LISTING

```
C     THIS DECK BELONGS TO BOB THOMPSON.
C     THIS PROGRAM SOLVES THE STEADY STATE POLYMERIZER PROBLEM FOR
C     THE NUMBER DENSITY FRACTIONS OF POLYMER PARTICLES HAVING UP TO
C     AND INCLUDING FIVE (5) FREE RADICALS GROWING SIMULTANEOUSLY.  THE
C     SYSTEM OF LINEAR FIRST ORDER DIFFERENTIAL EQUATIONS ARE TO BE
C     SOLVED BY A RUNGE-KUTTA TECHNIQUE BEGINNING AT THE SIZE OF A
C     MICELLE AND INTEGRATING ALONG THE PARTICLE VOLUME AXIS.
C
C     PROGRAM BEGUN DECEMBER 29, 1974.
C
      IMPLICIT REAL*8(A-Z)
      COMMON X00,X10,X20,X30,X40,X50,X0,X1,X2,X3,X4,X5,A1,A2,A3,A4,A5,A6
      COMMON A7,DZ,B,DH,Z,X60,X70,X80,X6,X7,X8,X90,X9,X110,X11
      INTEGER J,L
C
C     DEFINE THE CONSTANTS.
C
      B = 0.500
      DZ = 0.0010
      DH = DZ/2.0
    9 READ 6, A4,A5,A6,A7
      IF (A4 .EQ. 0.00)  GO TO 25
      READ 7,Z,X00,X10,X20,X30,X40,X50,AREA,NAREA
      READ 1000,  X60,X70,X80,X90,X110
      J = 0
      L = 0
      A1 = A6/A5
      A2 = A7/A5
      A3 = A4/A5
C
C     PRINT PRELIMINARY RESULTS.
C
      PRINT 1
      PRINT 2, DZ
      PRINT 175
      PRINT 200, A1,A2,A3,A4,A5,A6,A7
```

```
C     INITIALIZE THE SYSTEM (AT ZERO VOLUME).
C
      IF (Z .GT. 1.00)  GO TO 8
      X00 = (A1+A3)/(1.0+A1+2.0*A3)
      X10 = (1.0+A3)/(1.0+A1+2.0*A3)
      X20 = 0.00
      X30 = 0.00
      X40 = 0.00
      X50 = 0.00
      X60 = 0.00
      X70 = 0.00
      X80 = 0.00
      X90 = 0.00
      X110 = 0.00
    8 XT0 = X00 + X10 + X20 + X30 + X40 + X50
      NXT0 = X10 + 2.0*X20 + 3.0*X30 + 4.0*X40 + 5.0*X50
      NBAR0 = NXT0/XT0
C
C     PRINT INITIAL CONDITIONS.

      PRINT 50
      PRINT 100
      PRINT 110, Z,X00,X10,X20,X30,X40,X50,X60,X70,X80,XT0,NBAR0
      PRINT 111,X90,X110
C
C     CARRY OUT FIRST INTEGRATION STEP.
C
      CALL RK(10)
      Z = Z + DZ
      X0 = ((A1*X1)/(Z**(1./3.))+(2.0*A2*X2)/Z)/(1.0+A3*(Z**(2./3.)))
      XT = X0+X1+X2+X3+X4+X5
      NXT = X1 + 2.0*X2 + 3.0*X3 + 4.0*X4 + 5.0*X5
      NBAR = NXT/XT
      DAREA = DH*(XT0 + XT)
      AREA = AREA + DAREA
      NAREA = NAREA + DH*(NXT0 + NXT)
      PRINT 110, Z,X0,X1,X2,X3,X4,X5,X6,X7,X8,XT,NBAR
```

```
      PRINT 111,X9,X11
      GO TO 15
C
C     CARRY OUT RUNGE-KUTTA INTEGRATION.
C
   10 CALL RK(1)
      Z = Z + DZ
      X0 = ((A1*X1)/(Z**(1./3.))+(2.0*A2*X2)/Z)/(1.0+A3*(Z**(2./3.)))
      XT = X0+X1+X2+X3+X4+X5
      NXT = X1 + 2.0*X2 + 3.0*X3 + 4.0*X4 + 5.0*X5
      NBAR = NXT/XT
      DAREA = DH*(XT0 + XT)
      AREA = AREA + DAREA
      NAREA = NAREA + DH*(NXT0 + NXT)
C
C     PRINT PARTICLE SIZE RESULTS.
C
   12 IF (L.EQ.99)GO TO 14
      L = L + 1
      GO TO 15
   14 PRINT 110, Z,X0,X1,X2,X3,X4,X5,X6,X7,X8,XT,NBAR
      PRINT 111,X9,X11
      L = 0
   15 IF (J .EQ. 999)  GO TO 16
      J = J + 1
      GO TO 17
   16 NBARS = NAREA/AREA
      PRINT 155,Z,AREA,NAREA,NBARS
      J = 0
C
C     CONTINUE THE INTEGRATION.
C
   17 IF (DAREA/AREA .LE. 1.0E-9)  GO TO 20
      X10 = X1
      X20 = X2
      X30 = X3
      X40 = X4
```

```
      X50 = X5
      X60 = X6
      X70 = X7
      X80 = X8
      X90 = X9
      X110 = X11
      XT0 = XT
      NBAR0 = NBAR
      NXT0 = NXT
      GO TO 10
   20 CONTINUE
      NBARS = NAREA/AREA
      PRINT 150, AREA, NAREA
      PRINT 160, NBARS
      GO TO 9
   25 PRINT 300
      PRINT 400
C
C     FORMAT STATEMENTS.
C
    1 FORMAT(1H1,T21,'-PRELIMINARY  RESULTS-',///)
    2 FORMAT(15X,'DELTA Z = ',F15.5,/)
    6 FORMAT(4E20.6)
    7 FORMAT(F8.1,4E15.6/2E15.6,2E20.7)
   50 FORMAT(//,T21,'-INTEGRATION RESULTS-')
  100 FORMAT(///,T6,'Z',T15,'X0',T26,'X1',T37,'X2',T48,'X3',T59,'X4',T70
     1,'X5',T81,'X6',T92,'X7',T103,'X8',T114,'XT',T124,'NBAR',/)
  110 FORMAT(1X,1PE9.3,1P11E11.4)
  111 FORMAT(T50,1P2E15.6)
  150 FORMAT(/,T20,'AREA = ',E20.7,T50,'NAREA = ',E20.7,/)
  155 FORMAT(/,2X,F8.1,T20,'AREA = ',E20.7,T50,'NAREA = ',E20.7,T80,'NBA
     1RS = ',1PE20.7,/)
  160 FORMAT(/,T20,'SYSTEM NBAR = ',E20.7,/)
  175 FORMAT(/,T9,'A1',T24,'A2',T39,'A3',T54,'A4',T69,'A5',T84,'A6',T99,
     1'A7')
  200 FORMAT(/,1P7E15.6,//)
  300 FORMAT(/////,T25,'PROBLEM FINISHED')
```

```
  400 FORMAT(1H1)
 1000 FORMAT(5E15.6)
      STOP
      END
C
C     RUNGE-KUTTA SUBPROGRAM BEGINS.
C
      SUBROUTINE RK(I)
      IMPLICIT REAL*8(A-Z)
      COMMON X00,X10,X20,X30,X40,X50,X0,X1,X2,X3,X4,X5,A1,A2,A3,A4,A5,A6
      COMMON A7,DZ,B,DH,Z,X60,X70,X80,X6,X7,X8,X90,X9,X110,X11
      INTEGER N,I
      Y0 = X00
      Y1 = X10
      Y2 = X20
      Y3 = X30
      Y4 = X40
      Y5 = X50
      Y6 = X60
      Y7 = X70
      Y8 = X80
      Y9 = X90
      Y11 = X110
      ZD = Z
      N = 1
    1 Z3 = ZD**(1./3.)
      Z6 = ZD**(2./3.)
      IF (I .EQ. 1)  GO TO 2
      FX1 = A4*Z6*Y0 - (A5+A4*Z6+A6/Z3)*Y1 + 2.0*A6*Y2/Z3 + 6.0*A7*Y3/ZD
      GO TO 3
    2 FX0 = ((A1*Y1)/Z3 + (2.0*A2*Y2)/ZD)/(1.0+A3*Z6)
      FX1 = A4*Z6*FX0-(A5+A4*Z6+A6/Z3)*Y1 + 2.0*A6*Y2/Z3 + 6.0*A7*Y3/ZD
    3 FX2 = -A5*Y2/2.0+A7*(6.0*Y4-Y2)/ZD+(A4*Z6/2.0)*(Y1-Y2)+(A6/(2.0*Z3
     1))*(3.0*Y3-2.0*Y2)
      FX3 = -A5*Y3/3.0+(A7/3.0)*(20.0*Y5-6.0*Y3)/ZD+(A4*Z6/3.0)*(Y2-Y3)+
     1(A6/(3.0*Z3))*(4.0*Y4-3.0*Y3)
      FX4 = -A5*Y4/4.0+A7*(7.5*Y6-3.0*Y4)/ZD+A4*Z6*(Y3-Y4)/4.0+A6*(5.0*Y
```

```
     15-4.0*Y4)/(4.0*Z3)
      FX5 = -A5*Y5/5.0+A7*(42.0*Y7-20.0*Y5)/(5.0*ZD)+A4*Z6*(Y4-Y5)/5.0
     1+A6*(6.0*Y6-5.0*Y5)/(5.0*Z3)
      FX6 = -A5*Y6/6.0+A7*(56.0*Y8-30.0*Y6)/(6.0*ZD)+A4*Z6*(Y5-Y6)/6.0
     1+A6*(7.0*Y7-6.0*Y6)/(6.0*Z3)
      FX7 = -A5*Y7/7.0+A7*(56.0*Y9-42.0*Y7)/(7.0*ZD)+A4*Z6*(Y6-Y7)/7.0+
     1A6*(8.0*Y8-7.0*Y7)/(7.0*Z3)
      FX8 = -A5*Y8/8.0+A7*(90.0*Y11-56.0*Y8)/(8.0*ZD)+A4*Z6*(Y7-Y8)/8.0
     1+A6*(9.0*Y9-8.0*Y8)/(8.0*Z3)
      FX9 = -A5*Y9/9.0-8.0*A7*Y9/ZD+A4*Z6*(Y8-Y9)/9.0+A6*(10.0*Y11-9.0*
     1Y9)/(9.0*Z3)
      FX11 = -A5*Y11/10.0-A7*9.0*Y11/ZD+A4*Z6*(Y9-Y11)/10.0-A6*Y11/Z3
      GO TO (4,5,6,7), N
    4 X1 = X10 + DZ*FX1/6.0
      X2 = X20 + DZ*FX2/6.0
      X3 = X30 + DZ*FX3/6.0
      X4 = X40 + DZ*FX4/6.0
      X5 = X50 + DZ*FX5/6.0
      X6 = X60 + DZ*FX6/6.0
      X7 = X70 + DZ*FX7/6.0
      X8 = X80 + DZ*FX8/6.0
      X9 = X90 + DZ*FX9/6.0
      X11 = X110 + DZ*FX11/6.0
      Y1 = X10 + DH*FX1
      Y2 = X20 + DH*FX2
      Y3 = X30 + DH*FX3
      Y4 = X40 + DH*FX4
      Y5 = X50 + DH*FX5
      Y6 = X60 + DH*FX6
      Y7 = X70 + DH*FX7
      Y8 = X80 + DH*FX8
      Y9 = X90 + DH*FX9
      Y11 = X110 + DH*FX11
      ZD = Z + DH
      N = 2
      GO TO 1
    5 X1 = X1 + DZ*FX1/3.0
```

```
      X2 = X2 + DZ*FX2/3.0
      X3 = X3 + DZ*FX3/3.0
      X4 = X4 + DZ*FX4/3.0
      X5 = X5 + DZ*FX5/3.0
      X6 = X6 + DZ*FX6/3.0
      X7 = X7 + DZ*FX7/3.0
      X8 = X8 + DZ*FX8/3.0
      X9 = X9 + DZ*FX9/3.0
      X11 = X11 + DZ*FX11/3.0
      Y1 = X10 + DH*FX1
      Y2 = X20 + DH*FX2
      Y3 = X30 + DH*FX3
      Y4 = X40 + DH*FX4
      Y5 = X50 + DH*FX5
      Y6 = X60 + DH*FX6
      Y7 = X70 + DH*FX7
      Y8 = X80 + DH*FX8
      Y9 = X90 + DH*FX9
      Y11 = X110 + DH*FX11
      N = 3
      GO TO 1
    6 X1 = X1 + DZ*FX1/3.0
      X2 = X2 + DZ*FX2/3.0
      X3 = X3 + DZ*FX3/3.0
      X4 = X4 + DZ*FX4/3.0
      X5 = X5 + DZ*FX5/3.0
      X6 = X6 + DZ*FX6/3.0
      X7 = X7 + DZ*FX7/3.0
      X8 = X8 + DZ*FX8/3.0
      X9 = X9 + DZ*FX9/3.0
      X11 = X11 + DZ*FX11/3.0
      Y1 = X10 + DZ*FX1
      Y2 = X20 + DZ*FX2
      Y3 = X30 + DZ*FX3
      Y4 = X40 + DZ*FX4
      Y5 = X50 + DZ*FX5
      Y6 = X60 + DZ*FX6
```

```
      Y7 = X70 + DZ*FX7
      Y8 = X80 + DZ*FX8
      Y9 = X90 + DH*FX9
      Y11 = X110 + DH*FX11
      ZD = Z + DZ
      N = 4
      GO TO 1
    7 X1 = X1 + DZ*FX1/6.0
      X2 = X2 + DZ*FX2/6.0
      X3 = X3 + DZ*FX3/6.0
      X4 = X4 + DZ*FX4/6.0
      X5 = X5 + DZ*FX5/6.0
      X6 = X6 + DZ*FX6/6.0
      X7 = X7 + DZ*FX7/6.0
      X8 = X8 + DZ*FX8/6.0
      X9 = X9 + DZ*FX9/6.0
      X11 = X11 + DZ*FX11/6.0
      RETURN
      END
C
C     END OF SUBROUTINE.
C
```